VOLTAGE AND CURRENT MODE MULTIFUNCTION FILTER DESIGN WITH CURRENT CONVEYORS

by

Mehmet Can BAYRAM

A thesis submitted to

The Graduate Institute of Sciences and Engineering

of

Fatih University

In partial fulfillment of the requirements for the degree of

Master of Science

in

Electronics Engineering

June 2006
Istanbul, Turkey

I certify that this thesis satisfies all the requirements as a thesis for the degree of Master of Science.

Prof. Dr. Muhammet KÖKSAL
Head of Department

This is to certify that I have read this thesis and that in my opinion it is fully adequate, in scope and quality, as a thesis for the degree of Master of Science.

Prof. Dr. Kemal FİDANBOYLU
Supervisor

Examining Committee Members

Prof. Dr. Muhammet KÖKSAL

Prof. Dr. Kemal FİDANBOYLU

Asst. Prof. Dr. Tuğrul YANIK

It is approved that this thesis has been written in compliance with the formatting rules laid down by the Graduate Institute of Sciences and Engineering.

Asst. Prof. Dr. Nurullah ARSLAN
Director

June 2006

VOLTAGE AND CURRENT MODE MULTIFUNCTION FILTER DESIGN WITH CURRENT CONVEYORS

Mehmet Can BAYRAM

M. S. Thesis - Electronics Engineering
June 2006

Supervisor: Prof. Dr. Kemal FİDANBOYLU

ABSTRACT

Current conveyors and current conveyor based active elements are having a big attention lately. This attention let them to be used in the applications in various designs of analog electronics like amplifiers, filters, impedance converters, gyrators, oscillators or more generally signal processing circuits.

In this thesis, we have focused on the experimental verification of voltage mode second order multiple input single output (MISO) filters and design of both voltage-mode and current-mode second-order filters using current conveyors. We have presented three voltage-mode MISO second-order filters using CCIIs and one current-mode multifunctional second-order filter using DO-CCCII.

The MISO filters and multifunction filter transfer functions are analyzed for both ideal and non-ideal cases. The validity of the voltage mode filters has been verified both experimentally and through PSPICE simulations. On the other hand, the validity of the current mode filter has been verified only through PSPICE simulation.

Keywords: Current Conveyors, Current-mode, Voltage-mode, Active filters, Multifunction filters, AD844.

AKIM TAŞIYICILAR KULLANARAK GERİLİM VE AKIM-MODLU ÇOK İŞLEVLİ FİLTRE TASARIMI

Mehmet Can BAYRAM

Yüksek Lisans Tezi – Elektronik Mühendisliği
Haziran 2006

Tez Yöneticisi: Prof. Dr. Kemal FİDANBOYLU

ÖZ

Son senelerde akım taşıyıcılar ve akım taşıyıcı tabanlı aktif elemanlara olan ilgi giderek artmaktadır. Bu ilgi alan aktif elemanların genellikle amplifilatörler, empedans çeviriciler, jiratörler, osilatörler ve özellikle işaret işleme devreleri gibi çeşitli analog elektronik devrelerdeki uygulamaları dahi kullanımına yol açmıştır.

Bu tezde, ikinci dereceden çok-girişli tek-çıkışlı gerilim-modlu filtrelerin deneysel gerçeklemesi ve gerilim-modlu ve akım-modlu ikinci dereceden çok fonksiyonlu filtre devrelerinin akım taşıyıcılarla tasarımı ele alınmıştır. CCII kullanarak üç adet ikinci dereceden çok-girişli tek-çıkışlı gerilim-modlu filtre devresi ve DO-CCCII kullanarak bir adet ikinci dereceden çok fonksiyonlu akım-modlu filtre devresi sunulmuştur.

Çok girişli-tek çıkışlı filtrelerin ve çok işlevli filtrelerin transfer fonksiyonları ideal ve ideal olamayan durumlarda analiz edilmiştir. Tüm Gerilim-modlu filtreler hem deneysel olarak hem de PSPICE simulasyon programıyla gerçeklenmiştir. Diğer taraftan Akım-modlu filtre yalnızca PSPICE devre simulasyon programı kullanılarak gerçeklenmiştir.

Anahtar Kelimeler: Akım taşıyıcılar, Akım-modu, Gerilim-modu, Aktif filtreler, Çok işlevli filtreler, AD844.

DEDICATION

To my parents

ACKNOWLEDGEMENT

Firstly I would like to thank my supervisor, Prof. Dr. Kemal FİDANBOYLU, for all of his support, his guidance, and insight throughout the research.

Secondly thanks for my colleague and good friend Mehmet SAĞBAŞ for his help and support in every second of my thesis.

Thirdly thanks go to Prof. Dr. Muhammet KÖKSAL, Eser ÖNER, and Nasıf EKİZ. Their constant source of entertainment made coming to work a pleasure on even the busiest days. I wish them all the best in their future endeavors.

Finally thanks for all the Bayram family members.

TABLE OF CONTENTS

LIST OF FIGURES

FIGURE

LIST OF TABLES

TABLE

LIST OF SYMBOLS AND ABBREVIATIONS

AP	All-pass
BJT	Bipolar Junction Transistor
BR	Band-reject (Notch Filter)
BP	Band-pass
CC	Current Conveyor
CCI	First Generation Current Conveyor
CCI+	Positive-Type First Generation Current Conveyor
CCI-	Negative-Type First Generation Current Conveyor
CCII	Second Generation Current Conveyor
CCII+	Positive-Type Second Generation Current Conveyor
CCII-	Negative-Type Second Generation Current Conveyor
CCCII	Second Generation Current Controlled Current Conveyor
CCCII+	Positive-Type Second Generation Current Controlled Conveyor
CCCII-	Negative-Type Second Generation Current Controlled Conveyor
CCIII	Third Generation Current Conveyor
CCIII+	Positive-Type Third Generation Current Conveyor
CCIII-	Negative-Type Third Generation Current Conveyor
CFOA	Current Feedback Operational Amplifier
CM	Current-Mode
CMOS	Complimentary Metal-Oxide Semiconductor
DO-CCII	Dual-Output Second Generation Current Conveyor
DO-CCCII	Dual-Output Second Generation Current Controlled Conveyor
FTFN	Four Terminal Floating Nullor
HP	High-pass
IC	Integrated Circuit
LP	Low-pass
MISO	Multiple-Input Single-Output

CHAPTER 1

INTRODUCTION

Since their introduction in 1968, the current conveyors have led to a great number of applications in various designs of analog electronics, like amplifiers, filters, impedance converters, gyrators, oscillators or more generally signal processing circuits (Smith and Sedra, 1968).

Current-mode circuits and related active components such as current conveyor (CC), operational trans-conductance amplifier (OTA), operational mirrored amplifier (OMA), current feedback operational amplifier (CFOA), four terminal floating nullor (FTFN) emerged as an important class of circuits with properties that enable them to rival their voltage-mode counterparts in wide range applications. A current-mode circuit may be taken to mean any circuit in which current is used as active variable in preference to voltage, either throughout the whole circuit or only in certain critical areas. A current-mode approach is not just restricted to current processing, but also offers certain important advantages when interfaced to voltage-mode circuits. The use of current, rather than voltage as the active parameter can result in higher usable gain, accuracy and band-width due to reduced voltage excursion at sensitive nodes (Toumazou et al., 1990).

Although, current-mode circuits have important advantages over their voltage-mode counterparts, voltage-mode circuits are attractive especially with current conveyors. Conventional voltage-mode circuits consist of operational amplifiers which have the disadvantage of severely reduced bandwidth at higher gain, because of the operational amplifiers fixed gain-bandwidth product (Wilson, 1990), (Kumar and Shukla, 1985).

Second order active filters using different kind of active elements are of great interest. Many active filters were proposed in the literature. In this thesis, we focus on the design of second order voltage-mode multifunction filters using second generation current conveyors and the design of second order current-mode multifunction filters using dual-output second generation current conveyors.

It is also important to realize active filters using minimum number of active and passive elements. In the literature, most of the circuits have been realized using minimum number of elements (Sagbas et al., 2005). In this thesis, we also present active filters using minimum number of active and passive elements. All voltage-mode circuits in the thesis were experimentally verified using the AD844 IC manufactured by Analog Devices. The AD844 IC is a commercially available, versatile, low cost active component providing an excellent combination of AC and DC performance. It combines high bandwidth and very fast large signal response with excellent DC performance. It is also free from the slew rate limitations inherent in traditional opamps and other current-feedback opamps. It can be used instead of traditional opamps, however its current feedback architecture results in much better AC performance and high linearity (Analog Devices, 1990). It is equivalent to a combination of a positive-type second generation current conveyor and a unity-gain voltage buffer (Svoboda et al., 1991).

This thesis has been separated into several chapters. In Chapter 2, the literature survey on current-mode, voltage-mode circuits and current conveyors are presented.

Chapter 3 presents a new voltage-mode multiple-input single-output multifunction (MISO) filter using a single negative type second generation current conveyor (CCII-). The proposed multifunction filter is verified both experimentally and through simulations. For experimental verification, the commercially available current feedback operational amplifier AD844 manufactured by Analog Devices is used. The simulations are carried out using the model parameters of AD844 from the built-in library of PSPICE simulation program. The circuit analysis and sensitivity calculations are performed for both ideal and non-ideal cases. This filter which possesses three-inputs and one-output can generate all biquadratic filtering functions of low-pass, high-pass, band-pass and band-reject at the output terminal by selecting different input signal combinations Experimental and simulation results for low-pass, band-pass, high-pass, and band-reject filter configurations are presented at the end of the chapter.

Chapter 4 presents the experimental verification of a voltage-mode multiple-input single-output multifunction filter using a single current conveyor proposed by Sagbas (Sagbas, 2003). The current conveyor is realized by a commercially available current feedback operational amplifier AD844 of Analog Devices. The experimental results are also compared with PSPICE simulations. Effect of the non-idealities and the sensitivity analysis of the proposed filter are also examined. The circuit uses one positive-type second generation current conveyor (CCII+), three resistors and two capacitors. The use of CCII+ simplifies the filter circuit configuration. This filter which possesses three-inputs and one-output can generate all biquadratic filtering functions of low-pass, high-pass, band-pass and band-reject at the output terminal by selecting different input signal combinations. Experimental and simulation results for low-pass, band-pass, and high-pass filter configurations are presented at the end of the chapter.

Chapter 5 presents the experimental verification of a voltage-mode multiple-input single-output multifunction filter using two current conveyors proposed by Sagbas et al. (Sagbas et al., 2005). The current conveyors are realized by commercially available current feedback operational amplifier AD844 of Analog Devices. The experimental results are also compared with PSPICE simulations. Effect of the non-idealities and the sensitivity analysis of the proposed filter are also examined. The circuit uses one positive-type second generation current conveyor (CCII+), one negative-type second generation current conveyor (CCII-), three resistors, and two capacitors. This filter which possesses three-inputs and one-output can generate all biquadratic filtering functions of low-pass, high-pass, band-pass and band-reject at the output terminal by selecting different input signal combinations. Experimental and simulation results for low-pass, band-pass, and high-pass filter configurations are presented at the end of the chapter.

Chapter 6 presents a new current-mode multifunction filter that realizes three basic filter functions at its high impedance outputs with minimum number of passive elements. The proposed filter consists of only two passive elements (two capacitors) and two dual-output second generation current controlled conveyors (DO-CCCIIs). It has a single-input and three high impedance outputs. Each output provides a different filter response, namely low-pass (LP), high-pass (HP), and band-pass (BP). The sensitivity analysis is performed for ideal and non-ideal filter configurations. The validity of the proposed filter is verified through PSPICE simulations.

Finally, conclusions for the thesis are presented in Chapter seven.

CHAPTER 2

LITERATURE SURVEY

2.1 HISTORICAL BACKGROUND

2.1.1 Voltage Mode Circuits

Voltage-mode circuits using conventional operational amplifier have the disadvantage of severely reduced bandwidth at higher gains, because of the op-amp's fixed gain-bandwidth product. This disadvantage can be eliminated by using current conveyors and current conveyor based active components (Wilson et al., 1990), (Kumar et al., 1985), (Wandsworth et al., 1990).

Recently, many single and multi-output voltage-mode universal biquadratic filters using current conveyors have been reported in the literature (Chang, 1997), (Chang et al., 1999), (Horng et al., 1996), (Horng et al., 1997), (Liu et al., 1997), (Ozoguz et al., 1996), (Horng, 2001), (Ozcan et al., 2003), (Horng, 2004). Some of these filters employ single current conveyors (Liu et al., 1991), (Chong et al., 1986), (Ozcan et al., 2003), some others use single negative type current conveyors (Terzioglu and Cicekoglu, 2004), (Tiliute, 2001), and some of them employ two positive-type second-generation current conveyors (CCII+) and one voltage follower (Chang et al., 1999), (Ozuguz et al., 1996). Other filter types reported in the literature use one positive-type second-generation current conveyor (CCII+), one negative-type second-generation current conveyor (CCII-) and two capacitors and three resistors (Horng et al., 1996), (Liu et al., 1997).

Recently, Liu et al. reported a voltage-mode filter which employs one CCII+, one CCII-, two capacitors and three resistors (Liu et al., 1997). Chang proposed a voltage-mode filter which employs three CCII+s, two capacitors and three resistors (Chang, 1997). Later, Chang and Tu presented a voltage-mode filter which employs two CCII+s, two capacitors and three resistors with orthogonal control of ω_o and Q (Chang et al., 1999). However, this filter has four inputs and its transfer function is very complex (Chang et al., 1999). Horng proposed a voltage-mode filter which employs three CCII+s, two capacitors and two resistors (Horng, 2001).

The above mentioned filters employ at least two current conveyors. Several of these kinds of circuits are proposed using up to ten current conveyors or current conveyor based active components in the literature, however they suffer from one or more of the following drawbacks: Some of them use an excessive number of active components (Horng, et al., 2004), (Chang et al., 2003), (Shah et al., 2003), (Weng et al.., 2000), (Chang et al., 1999), (Horng et al., 2000), (Minaei et al., 2005), (Tangsrirat et al., 2005), (Horng et al., 2005), (Shah et al.,2003), (Shah et al., 2005). Since power consumptions are important for the circuit designers, they look for simple structures employing no more than a single active element. Some others use large number of passive components (Sharma et al., 2003), (Hou et al., 1999), (Horng et al., 2002), (Horng, 2004), (Weng et al., 2000), (Chang et al., 1999), (Tangsrirat et al., 2005), (Horng et al., 2005), (Shah. et al., 2005). Some of them do not realize all of the basic filter functions (Sharma et al., 2003), (Hou et al., 1999), (Özcan et al., 2003), (Horng et al., 2004), (Chang et al., 1999), (Minaei et al., 2005). Some others require extra inverting-type input signals for realizing filter functions (Özcan et al., 2003), (Horng, 2004), (Horng, 2003), (Horng, 2000). Some need high number of inputs and/or outputs, which imply high complexity (Horng et al., 2002), (Shah et al., 2005). Some of them are open loop circuits. It is well known that open loop circuits have disadvantages over their counterpart close loop circuits (Sharma et al., 2003), (Özcan, et al., 2003). Some others are lack of electronic tunability property (Sharma, et al., 2003), (Özcan et al., 2003), (Horng et al., 2002), (Shah et al., 2005), (Horng et al., 2004), (Horng, 2004), (Chang et al., 2003), (Horng, 2003), (Shah et al., 2003), (Chang et al., 1999), (Tangsrirat et al., 2005), (Shah et al., 2005).

2.1.2 Current Mode Circuits

The operational amplifier has served as the basic building block in analogue circuit design with the introduction of integrated circuits. Since then, the performance requirements for analogue circuits have changed after new integrated analogue circuit applications have appeared. Voltage-mode operational amplifier circuits have limited bandwidth at high closed-loop gains due to the constant gain-bandwidth product. Furthermore, the limited slew-rate of the operational amplifier affects the large-signal, high-frequency operation. When wide bandwidth, low power consumption and low voltage operation are needed simultaneously, the voltage-mode operational amplifier becomes too complex and has characteristics that are not needed, for example DC accuracy (Toumazou et al., 1990).

One procedure for finding alternative, preferably simpler circuit realizations is to use current signals rather than voltage signals for signal processing.

The use of current, rather than voltage as the active parameter can result in higher usable gain, accuracy and bandwidth due to the reduced voltage excursion at sensitive nodes.

Current-mode circuits have become very attractive due to some important advantages in comparison with their counterpart voltage-mode circuits. Some of these advantages are: wider bandwidth, lower power consumption, greater linearity and wider dynamic range (Toumazou et al., 1990).

Thus, a number of circuit realizations for universal current mode filters were proposed (Chang and Chen, 1991a), (Chang et al., 1994). These circuits suffer from one or more of the following drawbacks:

- Lack of electronic adjustability (Chang and Chen, 1991b), (Soliman, 1995), (Abuelma'atti and Shabra, 1996), (Chang, 1997).
- The use of one or more floating resistors and capacitors (Chang, 1997), (Senani, 1996), (Ozoguz and Acar, 1997).
- The use of an excessive number of current conveyors of different types (Senani, 1996), (Abuelma'atti and Khan, 1995), (Chang, 1993b), (Sun and Fidler, 1994), (Papazoglou and Karybakas, 1997).
- The need of additional current conveyors for realizing band reject response (Soliman, 1995), (Abuelma'tti and Khan, 1995), (Chang, 1993c).

- The necessity of changing the topology of the circuit which implies that the basic filter functions (low-pass, high-pass, and band-pass) can not be simultaneously realized (Hou and Wu, 1997).
- The use of three inputs and one output, which implies that only one filter function can be realized at a time (Chang et al., 1994), (Chen, 1991), (Chang, 1997).

The most important current mode devices are: The current feedback operational amplifier, the current-conveyor with its various subclasses developed in the last few years and the current follower. Nowadays, almost all the known circuits have current-mode implementations using these devices, starting from amplifiers, active filters, oscillators, precision rectifiers, voltage regulators and so on (Chong and Smith, 1986), (Chiu, 1996), (Becvar, 2000).

Current conveyors, introduced in the early 1970's, are now emerging as an important class of circuits which have a great number of applications in the various designs of analog electronics, such as amplifiers, filters, impedance converters, gyrators, oscillators or more generally signal processing circuits (Toumazou et al., 1990).

The first generation current conveyor (CCI) was introduced by Smith and Sedra in 1968 (Smith and Sedra, 1968). However CCI had distortion and accuracy limitations due to base current errors and output impedance restrictions (Wandsworth, 1990). Hence, in 1970 Sedra and Smith presented a more useful element, which was named as second generation current conveyor (CCII) (Smith and Sedra, 1970).

An improved version of second generation current controlled conveyor (CCCII) was introduced by Fabre et al. in 1995 (Fabre et al., 1995). Several other active filters operating in current-mode were presented in literature (Chang, 1993b), (Sun and Jefferis, 1998).

In the previous decade, different types of of circuits using current conveyors were realized (Teumazou et al., 1990), (Fabre, 1995), (Kuntman et al., 2000). Biquadratic current-mode active filter circuits including single current conveyors make up an important part of these circuits. It is very important to realize universal active filters with minimum number of active and passive elements.

Second generation current conveyors (CCII) were found very useful in filtering applications. Second-order active filters with infinite output impedance are of great interest because several cells of this kind can be directly connected in cascade to implement higher-order filters (Higashimura, 1991), (Soliman, 1996).

Although CCIIs have a great number of applications in various design of analog electronics, such as amplifiers, filters, impedance converters, gyrators, oscillators or more generally signal processing circuits (Hou et al., 1993), (Liu et al., 1990), they lack electronic adjustability. However, many applications require electronic adjustability. In particular, sophisticated techniques of signal processing require the ability to adapt filter characteristics extensively (Kwan and Martin, 1991). In such cases, it is desirable to vary filter coefficients electronically.

In current-mode circuits, transconductors (OTA) are used for performing the tuning operation (Khan and Ahmet, 1987), (Abuelma'atti et al., 1998). These are flexible and robust commercial devices which are able to provide a transconductance variation over a wide range. However, the non-virtually zero voltage which exists between the input terminals of the OTAs is a considerable drawback in filter design (Papazoglou and Karybakas, 1997).

By using the second generation current controlled conveyor (CCCII) introduced by Fabre et al. in 1995, current conveyor applications can be made electronically adjustable. Several active filters using this feature have been presented in the literature (Sun and Jefferis, 1998), (Chang, 1993a).

Minaei and Turkoz proposed a new current mode current controlled universal filter using four single-output current controlled conveyors and two grounded capacitors in 2000 (Minaei and Turkoz, 2000).

In 2000, Khan and Maheshwari, proposed new first order all-pass section using CCCII which uses two resistors and two capacitors. Although, this circuit provides electronic adjustability of the pole frequency, it works only in the voltage-mode (Khan and Maheshwari, 2000).

Minaei and Turkoz have proposed a new current mode current controlled universal filter using four single-output current controlled conveyors and three grounded capacitors in 2001 (Minaei and Turkoz, 2001). The proposed filter can simultaneously realize low-pass, band-pass and high-pass responses at high output impedance. The circuit provides independent control of the parameters ω_O and ω_O/Q

by adjusting the bias current of the CCCIIs, without disturbing the gains of the low-pass, band-pass and high-pass responses. In the same year, Minaei et al (Minaei et al., 2001) proposed a new second order band-pass, low-pass and high-pass filters using only one or two current controlled conveyors.

Recently, Sagbas and Fidanboylu have also proposed a new electronically tunable universal filter with single-input, triple-output employing only four elements (two capacitors and two negative-type second generation current controlled conveyors (CCCII)) (Sagbas and Fidanboylu, 2004). The proposed filter realizes three basic filter functions simultaneously: lowpass, highpass and bandpass.

2.1.3 Multifunction Current-Mode and Voltage-Mode Circuits

Voltage-mode and current mode filters have been classified in the literature into three categories.

(i) Single-input and single-output filters (Chang and Chen, 1991b), (Sun and Fidler, 1994).

(ii) Single-input and multi-output filters (Senani, 1992), (Chang, 1993a).

(iii) Multi-input and single-output filters (Chang and Chen, 1991a), (Chang, 1997).

Single-input and multi-output filters usually have two or three outputs and can implement two or more different filter functions simultaneously. The general form of their input-output transfer functions are as follows: $V_{O1} = f_1(V_i)$, $V_{O2} = f_2(V_i)$, $V_{O3} = f_3(V_i)$, etc. Several voltage-mode and current-mode single-input and multi-output multifunction filters were proposed in the literature (Singh and Senani, 1990), (Chang, 1993a), (Papazogluo and Karybakas, 1997).

Singh and Senani proposed a single-input, triple-output voltage-mode multifunction filter which employed three current conveyors (Singh and Senani, 1990). It gave the basic filter responses such as low-pass, band-pass and high-pass. Band-reject response was also obtained by selecting different output signal combinations.

Later, Chang proposed five different single-input and multi-output voltage-mode multifunction filters (Chang, 1997).

Papazoglou and Karybakas proposed electronically tunable single-input and triple-output current-mode multifunction filter (Papazogluo and Karybakas, 1997).

Chang proposed single-input and double-output current-mode multifunction filter which employed two current conveyors (Chang, 1993a). The outputs of the circuit did not have a high impedance, so it was not cascadable.

Multi-input and single-output filters have slightly different characteristics than the single-input filters. The general form of their input-output function is as follows: $V_O = f(V_1, V_2, V_3, ...)$. Different type of filter functions can be obtained by applying the signal to some inputs and by grounding the rest.

Many voltage-mode and current mode multi-input and single-output multifunction filters were proposed in the literature (Chang et al., 1994), (Horng et al., 1996), (Ozoguz and Gunes, 1996), (Horng et al., 1997), (Liu and Lee, 1997).

Chang and Lee proposed multi-input and single-output voltage-mode multifunction filter which employed three current conveyors and one current follower (Chang and Lee, 1996). Horng, et al. proposed the same configuration using one negative-type current conveyor, one positive-type current conveyor and one current follower (Horng et al., 1996).

As it can be seen from the above mentioned references, there has been a great emphasis on the design and implementation of filter design using current conveyors.

2.2 CURRENT CONVEYORS

A current conveyor is a four terminal device which when arranged with other electronic elements in specific circuit configurations can perform many useful analog signal processing functions (Smith and Sedra, 1968,), (Smith and Sedra, 1970). A Current conveyor received great attention in recent years as an alternative active element to classical voltage-mode operational amplifiers. The reason is mainly due to the commercial availability of current conveyor components as integrated circuits (Wandsworth, 1990). In voltage-mode circuit the input-output variables are voltages and in current-mode circuits they are currents. The classical operational amplifier with its high input impedance and low output impedance is a suitable element for voltage-mode circuits. However, the current conveyor has one high input impedance (ideally infinite), one low input impedance (ideally zero) and one high output impedance. These properties makes the current conveyor a suitable element for both voltage-mode and current-mode applications.

In mathematical terms, the current conveyor is described by the following hybrid equations:

$$\begin{bmatrix} V_x \\ I_y \\ I_z \end{bmatrix} = \begin{bmatrix} 1 & 0 & 0 \\ 0 & m & 0 \\ 0 & k & 0 \end{bmatrix} \begin{bmatrix} V_y \\ I_x \\ V_z \end{bmatrix} \quad (2.2.1)$$

Where, the generation of the current conveyor is determined by m and the symbol k determines the polarity of the conveyor. Types and generations of current conveyor is shown in Table 2.1

Table 2.1 Current conveyor generations and types.

	m	**k**
Positive type first generation current conveyor **(CCI+)**	1	1
Negative type first generation current conveyor **(CCI-)**	1	-1
Positive type second generation current conveyor **(CCII+)**	0	1
Negative type second generation current conveyor **(CCII-)**	0	-1
Positive type third generation current conveyor **(CCIII+)**	-1	1
Negative type third generation current conveyor **(CCIII-)**	-1	-1

2.2.1 First Generation Current Conveyor (CCI)

The first generation current conveyor (CCI) was introduced by Smith and Sedra in 1968 (Smith and Sedra, 1968). It is a 3-port device whose block diagram representation can be seen in Fig. 2.1.

In mathematical terms, CCI is described by the following hybrid equation

$$\begin{bmatrix} V_x \\ I_y \\ I_z \end{bmatrix} = \begin{bmatrix} 1 & 0 & 0 \\ 0 & 1 & 0 \\ 0 & \pm 1 & 0 \end{bmatrix} \begin{bmatrix} V_y \\ I_x \\ V_z \end{bmatrix} \quad (2.2.2)$$

Taking the non-idealities of the CCI into account, the above hybrid equation can be rewritten as

$$\begin{bmatrix} V_x \\ I_y \\ I_z \end{bmatrix} = \begin{bmatrix} \beta & 0 & 0 \\ 0 & 1 & 0 \\ 0 & \pm\alpha & 0 \end{bmatrix} \begin{bmatrix} V_y \\ I_x \\ V_z \end{bmatrix} \tag{2.2.3}$$

where, $\beta = 1 - \varepsilon_V$ and $\alpha = 1 - \varepsilon_i$. ε_V ($|\varepsilon_V| << 1$) and ε_i ($|\varepsilon_i| << 1$) denote the voltage and current tracking errors, respectively. In Eq. (2.2.2) and Eq. (2.2.3) the positive sign denotes a positive-type first generation current conveyor (CCI+) and the negative sign denotes a negative-type first generation current conveyor (CCI-).

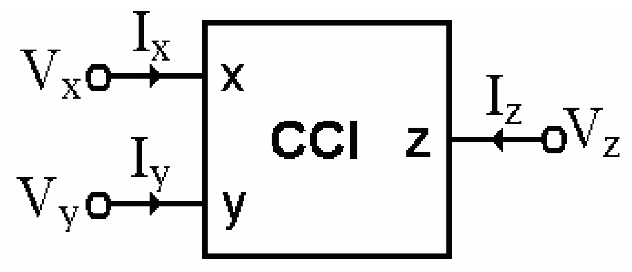

Figure 2.1 Block diagram of a first generation current conveyor.

2.2.2 Second Generation Current Conveyor (CCII)

To increase the versatility of the current conveyor, a second generation in which no current flows in terminal *y,* was introduced by Smith and Sedra in 1970. This building block has since proven to be more useful than CCI. Utilizing the block diagram representation of Fig. 2.2, (Smith and Sedra, 1970), CCII is described by following hybrid equation

$$\begin{bmatrix} V_x \\ I_y \\ I_z \end{bmatrix} = \begin{bmatrix} 1 & 0 & 0 \\ 0 & 0 & 0 \\ 0 & \pm 1 & 0 \end{bmatrix} \begin{bmatrix} V_y \\ I_x \\ V_z \end{bmatrix} \tag{2.2.4}$$

Taking the non-idealities of the CCI into account, the above terminal equations can be rewritten as

$$\begin{bmatrix} V_x \\ I_y \\ I_z \end{bmatrix} = \begin{bmatrix} \beta & 0 & 0 \\ 0 & 0 & 0 \\ 0 & \pm\alpha & 0 \end{bmatrix} \begin{bmatrix} V_y \\ I_x \\ V_z \end{bmatrix} \tag{2.2.5}$$

where, $\beta = 1 - \varepsilon_V$ and $\alpha = 1 - \varepsilon_i$. ε_V ($|\varepsilon_V| << 1$) and ε_i ($|\varepsilon_i| << 1$) denote the voltage and current tracking errors, respectively. In Eq. (2.2.4) and Eq. (2.2.5) the positive sign denotes a positive-type second generation current conveyor (CCII+) and the negative sign denotes a negative-type second generation current conveyor (CCII-).

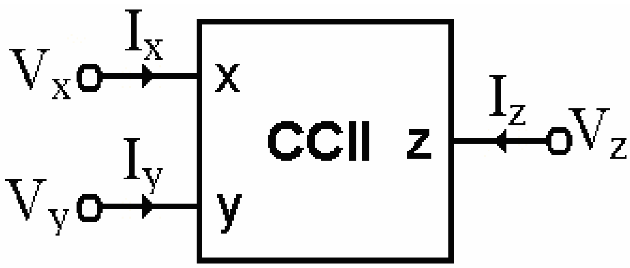

Figure 2.2 Block diagram of a second generation current conveyor.

CCII has three terminals; terminal *y* of the second generation current conveyor exhibits infinite input impedance. The voltage at terminal *x* follows that applied to the voltage terminal *y*, thus terminal *x* exhibits zero input impedance. The current supplied to terminal *x* is conveyed to the high-impedance output terminal *z* which can be supplied with either positive polarity or negative polarity.

CCIIs have wide application areas such as the realization of controlled sources, impedance converters, impedance inverters, gyrators, oscillators, and various analog computational elements like current amplifiers, current differentiators, current integrators, current summers and weighted current summers. A great deal of work has been reported on the realization of the voltage-mode and current-mode filters (Sun and Fidler, 1994), (Horng, 2001).

Schematic implementation for the positive-type and negative-type CCIIs, using BJT technology is shown in Fig. 2.3 and Fig 2.4, respectively, (Smith and Sedra, 1970).

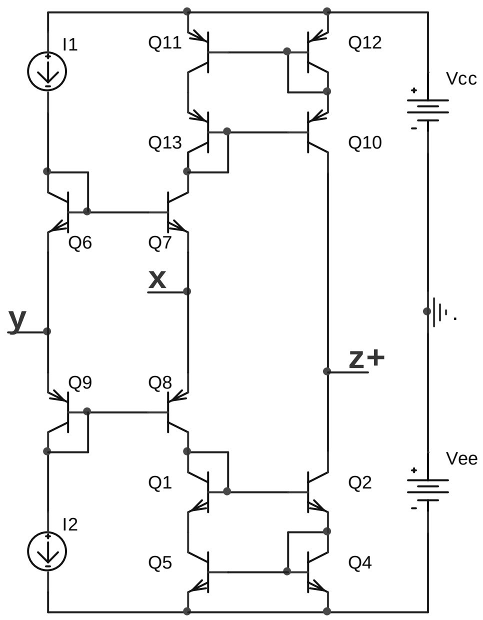

Figure 2.3 Schematic implementation for positive-type second generation current conveyor (CCII+) using BJT technology.

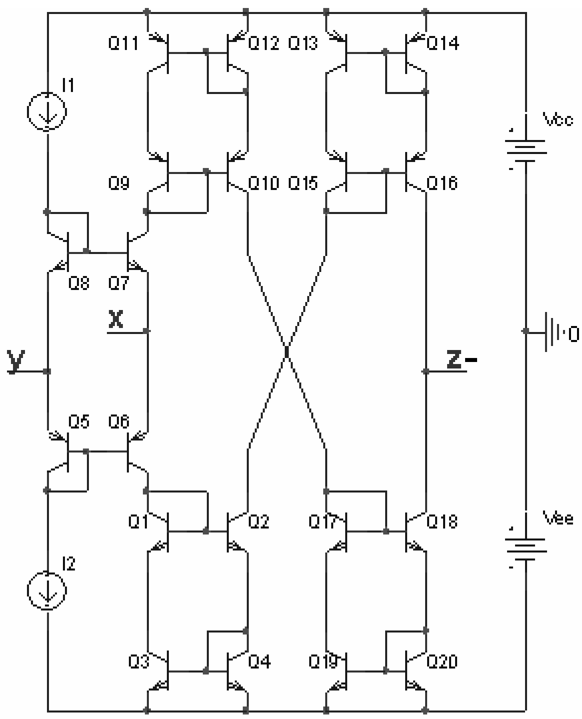

Figure 2.4 Schematic implementation for negative-type second generation current conveyor (CCII-) using BJT technology.

2.2.3 Dual-Output Second Generation Current Conveyor (DO-CCII)

The dual-output second generation current conveyor (Soliman, 1997) also called four terminal active current conveyor (CFCCII) (Gunes and Anday, 1996) which is shown in Figure 2.5 is defined by the following hybrid equations:

$$\begin{bmatrix} V_x \\ I_y \\ I_{z+} \\ I_{z-} \end{bmatrix} = \begin{bmatrix} 0 & 1 & 0 & 0 \\ 0 & 0 & 0 & 0 \\ 1 & 0 & 0 & 0 \\ -1 & 0 & 0 & 0 \end{bmatrix} \begin{bmatrix} I_x \\ V_y \\ V_{z+} \\ V_{z-} \end{bmatrix} \tag{2.2.6}$$

The input impedances for the ideal DO-CCII are infinite at terminal *y* and zero at terminal *x*, respectively. The terminal *z*, that is equivalent to a current generator, possesses infinite output impedance.

This active element has been used in other application (Ikeda and Tomita, 1994). Bipolar and CMOS realizations for the DO-CCII are presented in (Ikeda and Tomita, 1994), (Elwan and Soliman, 1996). Schematic implementation for negative type CCCII using BJT technology is shown in Fig. 2.6.

Taking the non-idealities of the DO-CCII into account, the above terminal equations can be rewritten as

$$\begin{bmatrix} V_x \\ I_y \\ I_{z+} \\ I_{z-} \end{bmatrix} = \begin{bmatrix} 0 & \beta & 0 & 0 \\ 0 & 0 & 0 & 0 \\ \alpha & 0 & 0 & 0 \\ -\alpha & 0 & 0 & 0 \end{bmatrix} \begin{bmatrix} I_x \\ V_y \\ V_{z+} \\ V_{z-} \end{bmatrix} \tag{2.2.7}$$

where $\beta = 1 - \varepsilon_v$ and $\alpha = 1 - \varepsilon_i$. ε_V $(|\varepsilon_V| << 1)$, ε_i $(|\varepsilon_i| << 1)$ denote the voltage and current tracking errors, respectively.

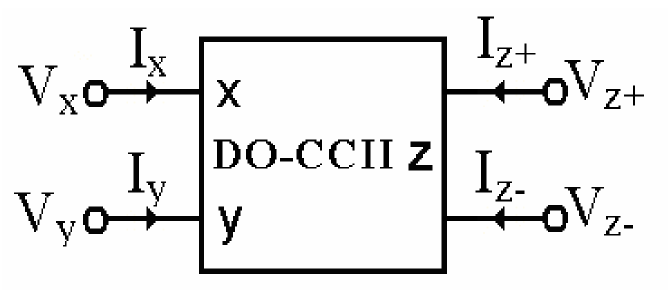

Figure 2.5 Block diagram of a dual-output second generation current conveyor.

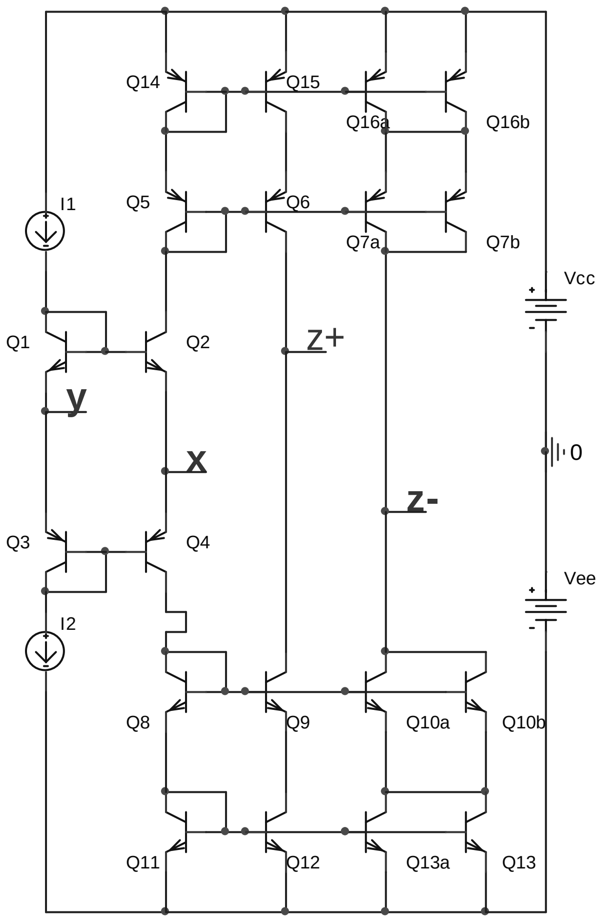

Figure 2.6 Schematic implementation for DO-CCII using BJT technology.

2.2.4 Third Generation Current Conveyor (CCIII)

The third generation current conveyor (CCIII) was presented by Fabre in 1995 (Fabre, 1995). This circuit picks up the current on a floating passive element. A CMOS implementation of CCII was presented by Piovaccari in 1995 (Piovaccari, 1995).

The third generation current conveyor is shown in Fig. 2.7 and its schematic implementation using CMOS technology is shown in Fig. 2.8. The terminal equations of the third generation current conveyor is given by

$$\begin{bmatrix} V_x \\ I_y \\ I_z \end{bmatrix} = \begin{bmatrix} 1 & 0 & 0 \\ 0 & -1 & 0 \\ 0 & \pm 1 & 0 \end{bmatrix} \begin{bmatrix} V_y \\ I_x \\ V_z \end{bmatrix} \qquad (2.2.8)$$

Taking the non-idealities of the CCIII into account, the above terminal equations can be rewritten as

$$\begin{bmatrix} V_x \\ I_y \\ I_z \end{bmatrix} = \begin{bmatrix} \beta & 0 & 0 \\ 0 & -1 & 0 \\ 0 & \pm\alpha & 0 \end{bmatrix} \begin{bmatrix} V_y \\ I_x \\ V_z \end{bmatrix} \tag{2.2.9}$$

where $\beta = 1-\varepsilon_v$ and $\alpha = 1-\varepsilon_i$. $\varepsilon_V\,(|\varepsilon_V| << 1)$, $\varepsilon_i\,(|\varepsilon_i| << 1)$ denote the voltage and current tracking errors, respectively.

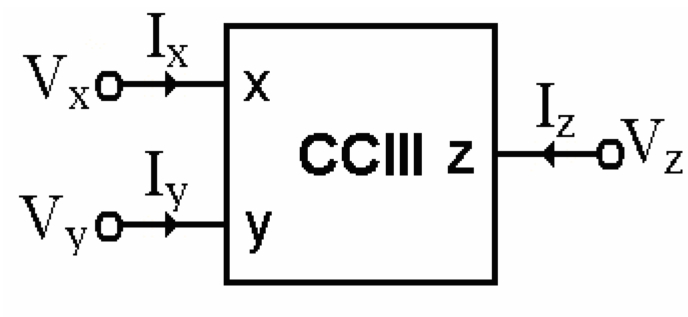

Figure 2.7 Block diagram of a third generation current conveyor (CCIII).

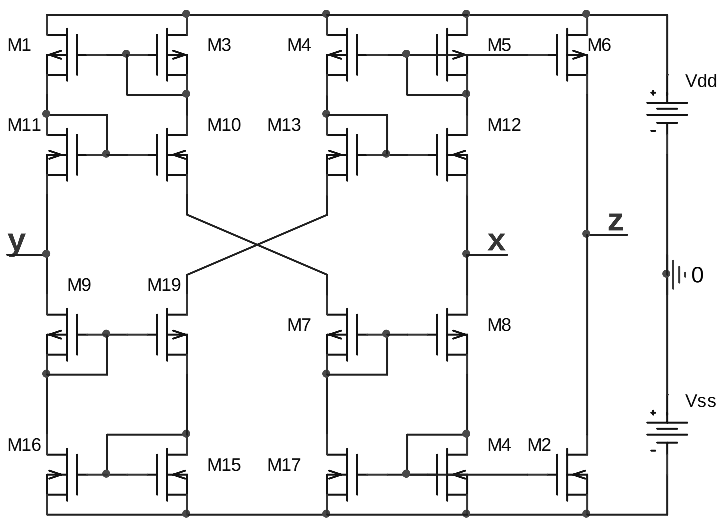

Figure 2.8 Schematic implementation for third generation current conveyor (CCIII) using CMOS technology.

2.3 THE AD844 OPERATIONAL AMPLIFIER

The AD844 is a high speed monolithic operational amplifier fabricated using Analog Devices' junction isolated complementary bipolar (CB) process. It combines high bandwidth and very fast large signal response with excellent dc performance. Although optimized for use in current to voltage applications and as an inverting mode amplifier, it is also suitable for use in many noninverting applications. The AD844 can be used in place of traditional op amps, but its current feedback architecture results in much better ac performance, high linearity and an exceptionally clean pulse response. This type of op amp provides a closed-loop bandwidth which is determined primarily by the feedback resistor and is almost independent of the closed-loop gain. The AD844 is relatively free from the slew rate limitations inherent in traditional op amps and other current-feedback op amps. Connection diagram of AD844A is shown in Fig. 2.9. (Analog Devices, 1990)

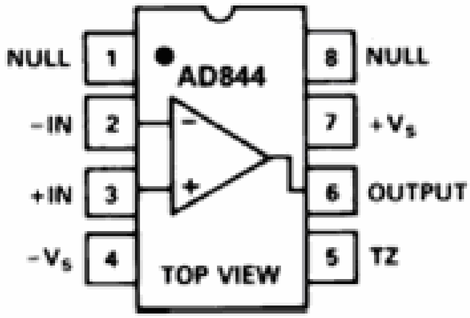

Figure 2.9 Connection Diagram of CFOA AD844/AD.

The AD844 op-amp has the following advantages:

(i) It is a versatile, low cost component providing an excellent combination of ac and dc performance (Analog Devices, 1990).

(ii) It is essentially free from slew rate limitations. Rise and fall times are essentially independent of output level (Analog Devices, 1990).

(iii) It can be operated from ±4.5 V to ±18 V power supplies and is capable of driving loads down to 50 Ω, as well as driving very large capacitive loads using an external network (Analog Devices, 1990).

(iv) The offset voltage and input bias currents are laser trimmed to minimize dc errors; VOS drift is typically 1 mV/°C and bias current drift is typically 9 nA/°C (Analog Devices, 1990).

(v) It exhibits excellent differential gain and differential phase characteristics, making it suitable for a variety of video applications with bandwidths up to 60 MHz (Analog Devices, 1990).

(vi) It combines low distortion, low noise and low drift with wide bandwidth, making it outstanding as an input amplifier for flash A/D converters. (Analog Devices, 1990)

CHAPTER 3

A NEW VOLTAGE MODE MULTIPLE INPUT SINGLE OUTPUT (MISO) FILTER USING A SINGLE NEGATIVE TYPE CURRENT CONVEYOR

3.1 INTRODUCTION

In this chapter, a new voltage-mode multiple-input single-output multifunction (MISO) filter using a single negative type second generation current conveyor (CCII-) is proposed. The proposed multifunction filter is verified both experimentally and through simulations. For experimental verification, the commercially available current feedback operational amplifier AD844 manufactured by Analog Devices was used. The simulations were carried out using the model parameters of AD844 from the built-in library of PSPICE simulation program. The circuit analysis and sensitivity calculations are performed for both ideal and non-ideal cases.

Recently, many MISO universal biquadratic filters using current conveyors or current conveyor based active elements have been reported in the literature. Some of these filters employ two positive type second generation current conveyors (CCII+s) and one voltage follower (Chang et al., 1999), (Ozoguz and Gunes, 1996). Some other filters employ one CCII+, one CCII-, and two capacitors and three resistors (Horng et al., 1996), (Liu et al., 1997).

The proposed circuit uses only one CCII-, two resistors and two capacitors. This filter, which possesses three-inputs and one-output can generate all biquadratic filtering functions of low-pass, high-pass, band-pass, band-reject, and all-pass at the output terminal by selecting different input signal combinations and has the following advantages over the ones proposed in literature.

(i) Voltage-mode circuits using conventional operational amplifier have the disadvantage of severely reduced bandwidth at higher gains because of the op-amp's fixed gain-bandwidth product. These disadvantages can be eliminated by using current conveyors and current conveyor based active elements (Wilson et al., 1990), (Wandsworth et al., 1990).

(ii) Realization of all the basic filter functions: low-pass, high-pass, band-pass, band-reject, and all-pass;

(iii) Low passive and active sensitivities.

(iv) Ability to adjust the natural frequency and quality factor.

(v) High quality factor

This chapter is divided into several sections. Section 3.2 presents circuit description and the analysis of the proposed multifunction filter for both ideal and non-ideal cases. In section 3.3, the sensitivity analysis of the proposed filter is presented. In section 3.4, the experimental and simulation results are presented.

3.2 CIRCUIT DESCRIPTION AND ANALYSIS OF THE PROPOSED FILTER

3.2.1 Ideal Case

The block diagram of a negative-type second generation current conveyor (CCII-) is shown in Fig. 3.1. The terminal equations for the ideal case can be written as (Smith et al., 1970)

$$I_y = 0 \tag{3.2.1}$$

$$V_x = V_y \tag{3.2.2}$$

$$I_z = -I_x . \tag{3.2.3}$$

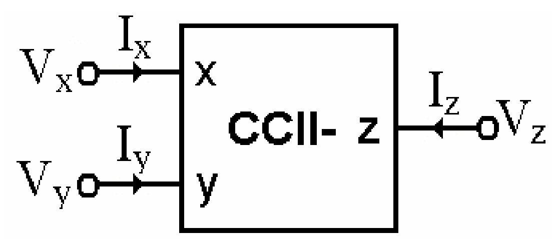

Figure 3.1 Block diagram of a negative type second generation current conveyor (CCII-).

The input impedances of the ideal CCII- are infinite at terminal *y* and zero at terminal *x*, respectively. The terminal *z*, that is equivalent to a current generator possesses infinite output impedance.

The proposed voltage mode MISO filter is shown in Fig.3.2. This circuit is analyzed using terminal equations given in Eqs. (3.2.1) through (3.2.3) as follows:

The input voltages can be written as

$$V_x = V_y = V_O . \tag{3.2.4}$$

Furthermore, the terminal currents can be written as

$$I_x = (V_1 - V_x)Y_1 = (V_1 - V_O)Y_1 \tag{3.2.5}$$

$$I_y = (V_4 - V_O)Y_3 + (V_2 - V_O)Y_2 \tag{3.2.6}$$

$$I_z = (V_3 - V_4)Y_4 + (V_O - V_4)Y_3 . \tag{3.2.7}$$

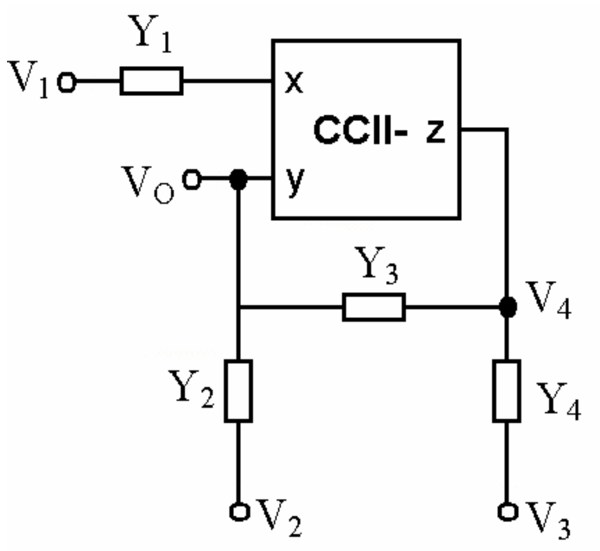

Figure 3.2 Circuit diagram of the proposed voltage-mode MISO multifunction filter.

Assuming that $I_y = 0$, then Eq. (3.2.6) becomes

$$(V_4 - V_O)Y_3 + (V_2 - V_O)Y_2 = 0 \tag{3.2.8}$$

Equation (3.2.8) can be simplified as follows:

$$V_4 = \frac{V_O(Y_2 + Y_3) - V_2 Y_2}{Y_3} \tag{3.2.9}$$

The terminal currents in Eqs. (3.2.5) and (3.2.7) can be equated using the relation given by Eq. (3.2.3). Hence, we obtain

$$(V_3 - V_4)Y_4 + (V_O - V_4)Y_3 = -(V_1 - V_O)Y_1 . \tag{3.2.10}$$

Equation (3.2.10) can be simplified as follows:

$$V_O(Y_3 - Y_1) = -V_1Y_1 - V_3Y_4 + V_4(Y_3 + Y_4) \tag{3.2.11}$$

Substituting Eq. (3.2.9) into Eq. (3.2.11), we obtain

$$V_O(Y_3 - Y_1) = -V_1Y_1 - V_3Y_4 + \left(\frac{V_O(Y_2 + Y_3) - V_2Y_2}{Y_3}\right)(Y_3 + Y_4) . \tag{3.2.12}$$

Equation (3.2.12) can be simplified as

$$V_O\left(Y_3 - Y_1 - \frac{(Y_2 + Y_3)(Y_3 + Y_4)}{Y_3}\right) = -V_1Y_1 - V_3Y_4 - \left(\frac{V_2Y_2}{Y_3}\right)(Y_3 + Y_4) \tag{3.2.13}$$

The transfer function of the proposed filter can be obtained by rearranging the terms in Eq. (3.2.13)

$$V_O = \frac{V_1(Y_1Y_3) + V_2(Y_2Y_3 + Y_2Y_4) + V_3(Y_3Y_4)}{Y_1Y_3 + Y_2Y_3 + Y_2Y_4 + Y_3Y_4} . \tag{3.2.14}$$

The admittance parameters are chosen as follows:

$$Y_1 = G_1 = \frac{1}{R_1} \tag{3.2.15a}$$

$$Y_2 = sC_2 \tag{3.2.15b}$$

$$Y_3 = G_3 = \frac{1}{R_3} \tag{3.2.15c}$$

$$Y_4 = sC_4 \tag{3.2.15d}$$

Hence, the transfer function of the proposed filter can be written as:

$$V_O = \frac{V_1(G_1G_3) + V_2(sC_2G_3 + s^2C_2C_4) + V_3(sG_3C_4)}{s^2C_2C_4 + s(C_2G_3 + G_3C_4) + G_1G_3}. \tag{3.2.16}$$

Special Cases:

(i) Low-pass (LP) filter realization:

In order to obtain a low-pass response from the MISO multifunction filter, the input signal is applied through the terminals V_1 while the terminals V_2 and V_3 are grounded. Hence, the transfer function given by Eq. (3.2.16) becomes as follows:

$$V_O = \frac{G_1G_3}{s^2C_2C_4 + s(C_2G_3 + G_3C_4) + G_1G_3}V_1 \tag{3.2.17}$$

The proposed circuit diagram which a gives low-pass filter response is shown in Fig. 3.3.

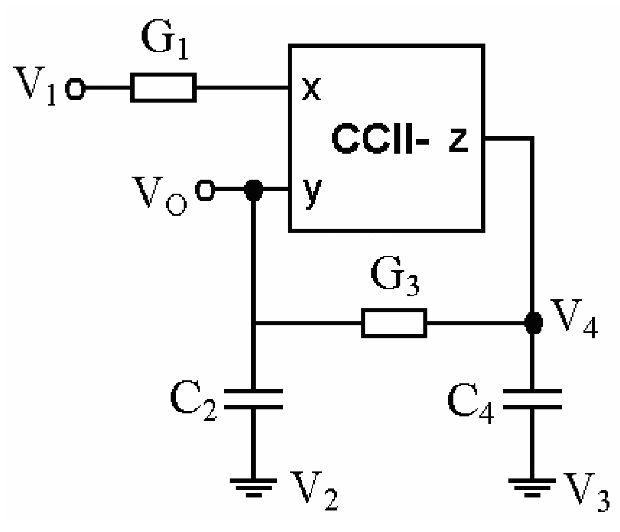

Figure 3.3 Proposed circuit diagram of the filter showing low-pass filter configuration.

(ii) High-pass (HP) filter realization:

In order to obtain a high-pass response from the MISO multifunction filter, the input signal is applied through the terminal V_2 and the inverse of the input signal is applied to V_3 while the terminal V_1 is grounded. Also passive components must be chosen as $C_2 = C_4$. Hence, the transfer function given by Eq. (3.2.16) becomes as follows:

$$V_O = \frac{s^2 C_2 C_4}{s^2 C_2 C_4 + s(C_2 G_3 + G_3 C_4) + G_1 G_3} V_2 \tag{3.2.18}$$

The proposed circuit diagram which gives a high-pass filter response is shown in Fig. 3.4.

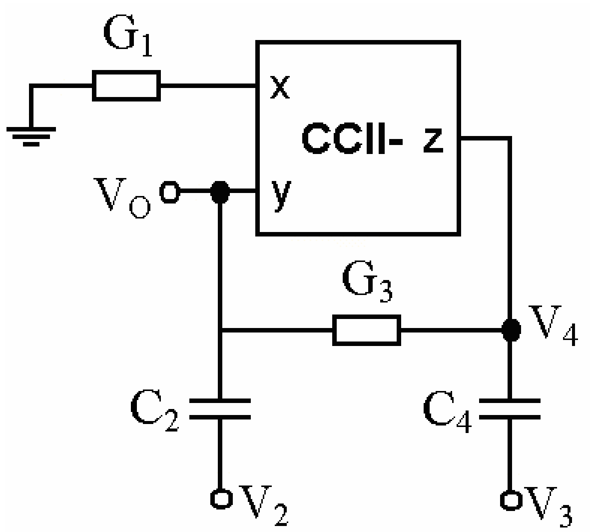

Figure 3.4 Proposed circuit diagram of the filter showing high-pass filter configuration.

(iii) Band-pass (BP) filter realization:

In order to obtain a band-pass response from the MISO multifunction filter, the input signal is applied through the terminal V_3 while the terminals V_1 and V_2 are grounded. Hence, the transfer function given by Eq. (3.2.16) becomes as follows:

$$V_O = \frac{sG_3C_4}{s^2C_2C_4 + s(C_2G_3 + G_3C_4) + G_1G_3} V_3 \quad (3.2.19)$$

The proposed circuit diagram which gives band-pass filter response is shown in Fig. 3.5.

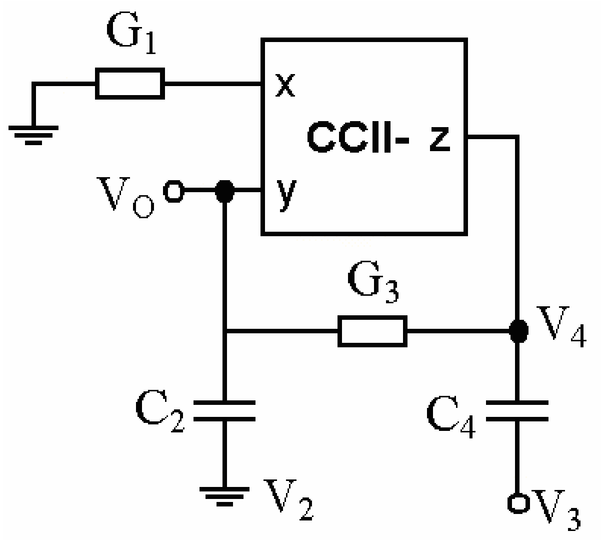

Figure 3.5 Proposed circuit diagram of the filter showing band-pass filter configuration.

(iv) Band-reject (BR) filter realization:

In order to obtain a band-reject response from the MISO multifunction filter, the input signal is applied through the terminals V_1 and V_2 while the terminal V_3 is grounded. Hence, the transfer function given by Eq. (3.2.16) becomes as follows:

$$V_O = \frac{s^2C_2C_4 + sC_2G_3 + G_1G_3}{s^2C_2C_4 + s(C_2G_3 + G_3C_4) + G_1G_3} V_1 \quad (3.2.20)$$

The proposed circuit diagram which gives band-reject filter response is shown in Fig. 3.6.

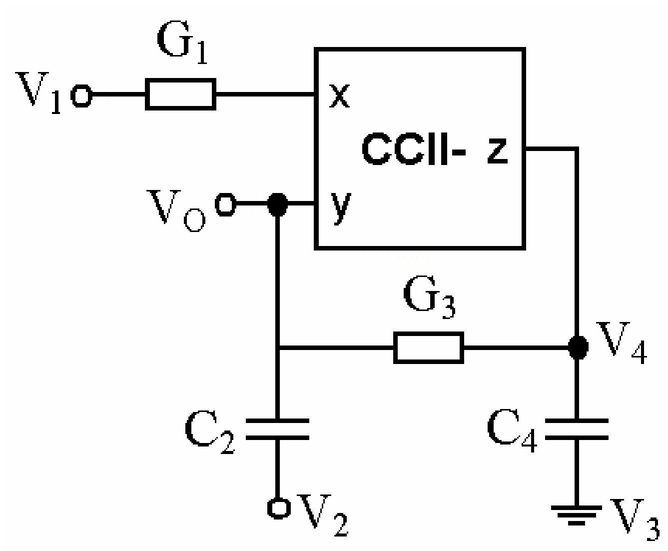

Figure 3.6 Proposed circuit diagram of the filter showing band-reject filter configuration.

(v) All-pass (AP) filter realization:

In order to obtain an all-pass response from the MISO multifunction filter, the input signal is applied through the terminals V_1, V_2 and V_3 with the following constraint:

$$V_1 = V_2 = \frac{V_3}{a},$$

where $a = -1 - \frac{2C_2}{C_4}$. If we choose $C_2 = C_4$, then $a = -3$. Hence, the transfer function given by Eq. (3.2.16) becomes as follows:

$$V_O = \frac{s^2 C_4{}^2 - 2sG_3C_4 + G_1G_3}{s^2 C_4{}^2 + 2sG_3C_4 + G_1G_3} V_1 \qquad (3.2.21)$$

The proposed circuit diagram which gives band-reject filter response is shown in Fig. 3.7.

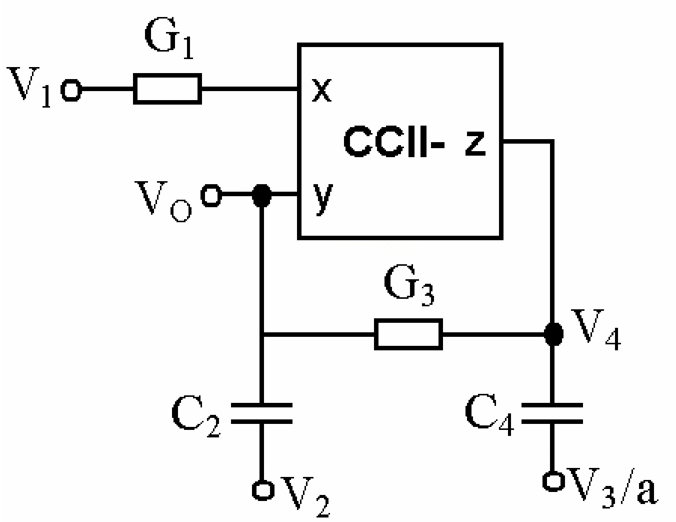

Figure 3.7 Proposed circuit diagram of the filter showing all-pass filter configuration.

From above analysis, it can be observed that all the standard filter functions namely; high-pass (HP), low-pass (LP), band-pass (BP), band-reject (BR) and all-pass (AP) can be obtained from the proposed filter. It is important to note that, in order to obtain the same natural frequency and quality factor for all filter characteristics, the same constraints for passive components must be chosen. The natural frequency and the quality factor of the proposed circuit are obtained from the denominator of the transfer function given in Eq. 3.2.16 as follows:

$$\omega_o = \sqrt{\frac{G_1 G_3}{C_2 C_4}} = \sqrt{\frac{1}{R_1 R_3 C_2 C_4}} \tag{3.2.22}$$

$$Q = \frac{\sqrt{G_1 G_3 C_2 C_4}}{G_3 C_4 + G_3 C_2} = \frac{\sqrt{R_3 C_2 C_4}}{\sqrt{R_1}(C_2 + C_4)} \tag{3.2.23}$$

3.2.2 Non-ideal Case

Taking the non-idealities into account, the terminal equations of the CCII- shown in Fig. 3.1 can be written as

$$I_y = 0 \tag{3.2.24}$$

$$V_x = \beta V_y \tag{3.2.25}$$

$$I_z = -\alpha I_x \tag{3.2.26}$$

where, $\beta = 1-\varepsilon_V$ and $\alpha = 1-\varepsilon_i$. ε_V ($|\varepsilon_V| << 1$) and ε_i ($|\varepsilon_i| << 1$) denote the voltage and current tracking errors, respectively (Smith et al., 1970).

Using Eq. (3.2.24) through (3.2.26), the terminal equations for the circuit shown in Fig. 3.2 become

$$V_y = V_O \tag{3.2.27}$$

$$\frac{V_x}{\beta} = V_y = V_O \tag{3.2.28}$$

$$I_x = (V_1 - V_x)Y_1 = (V_1 - \beta V_O)Y_1 \tag{3.2.29}$$

$$I_y = (V_4 - V_O)Y_3 + (V_2 - V_O)Y_2 \tag{3.2.30}$$

$$I_z = (V_3 - V_4)Y_4 + (V_O - V_4)Y_3 . \tag{3.2.31}$$

Assuming that $I_y = 0$, then Eq. (3.2.30) becomes

$$(V_4 - V_O)Y_3 + (V_2 - V_O)Y_2 = 0 . \tag{3.2.32}$$

Eq. (3.2.32) can be simplified as follows:

$$V_4 = \frac{V_O(Y_2 + Y_3) - V_2 Y_2}{Y_3} \tag{3.2.33}$$

Applying the relation given by Eq. (3.2.26) to Eqs. (3.2.29) and (3.2.31), we obtain

$$(V_3 - V_4)Y_4 + (V_O - V_4)Y_3 = -\alpha(V_1 - \beta V_O)Y_1 \tag{3.2.34}$$

Equation (3.2.34) can be simplified as

$$V_O(Y_3 - \alpha\beta Y_1) = -\alpha V_1 Y_1 - V_3 Y_4 + V_4(Y_3 + Y_4) \tag{3.2.35}$$

Substituting Eq. (3.2.33) into Eq. (3.2.35), we obtain

$$V_O(Y_3 - \alpha\beta Y_1) = -\alpha V_1 Y_1 - V_3 Y_4 + \left(\frac{V_O(Y_2 + Y_3) - V_2 Y_2}{Y_3}\right)(Y_3 + Y_4)\,. \tag{3.2.36}$$

Eq. (3.2.36) can be simplified as follows:

$$V_O\left(Y_3 - \alpha\beta Y_1 - \frac{(Y_2 + Y_3)(Y_3 + Y_4)}{Y_3}\right) = -\alpha V_1 Y_1 - V_3 Y_4 - \left(\frac{V_2 Y_2}{Y_3}\right)(Y_3 + Y_4) \tag{3.2.37}$$

The transfer function of the proposed filter taking the non-ideal effects into account becomes;

$$V_O = \frac{\alpha V_1(Y_1 Y_3) + V_2(Y_2 Y_3 + Y_2 Y_4) + V_3(Y_3 Y_4)}{\alpha\beta Y_1 Y_3 + Y_2 Y_3 + Y_2 Y_4 + Y_3 Y_4}\,. \tag{3.2.38}$$

Substituting the admittance parameters given by Eqs. (3.2.15a) through (3.2.15d), into equation (3.2.38), we obtain

$$V_O = \frac{\alpha V_1(G_1 G_3) + V_2(sC_2 G_3 + s^2 C_2 C_4) + V_3(sG_3 C_4)}{s^2 C_2 C_4 + s(C_2 G_3 + G_3 C_4) + \alpha\beta G_1 G_3}\,. \tag{3.2.39}$$

The non-ideal natural frequency and the quality factor of the proposed filter are obtained from the denominator of the transfer function given in Eq. (3.2.39) as follows:

$$\omega_o = \sqrt{\frac{\alpha\beta G_1 G_3}{C_2 C_4}} = \sqrt{\frac{\alpha\beta}{R_1 R_3 C_2 C_4}} \tag{3.2.40}$$

$$Q = \frac{\sqrt{\alpha\beta G_1 G_3 C_2 C_4}}{G_3 C_4 + G_3 C_2} = \frac{\sqrt{\alpha\beta R_3 C_2 C_4}}{\sqrt{R_1}\,(C_2 + C_4)}\,. \tag{3.2.41}$$

3.3 SENSITIVITY ANALYSIS

The ideal sensitivities of the natural frequency and the quality factor with respect to passive components are calculated using Eqs. (3.2.22) and (3.2.23) as follows:

$$S_{G_1}^{\omega_o} = S_{G_3}^{\omega_o} = \frac{1}{2} \tag{3.3.1}$$

$$S_{C_2}^{\omega_o} = S_{C_4}^{\omega_o} = S_{R_1}^{\omega_o} = S_{R_3}^{\omega_o} = -\frac{1}{2} \tag{3.3.2}$$

$$S_{G_1}^{Q} = S_{R_3}^{Q} = \frac{1}{2} \tag{3.3.3}$$

$$S_{G_3}^{Q} = S_{R_1}^{Q} = -\frac{1}{2} \tag{3.3.4}$$

$$S_{C_2}^{Q} = \frac{1}{2} - \frac{C_2}{C_2 + C_4} \tag{3.3.5}$$

$$S_{C_4}^{Q} = \frac{1}{2} - \frac{C_4}{C_2 + C_4}\ . \tag{3.3.6}$$

If the passive component values are chosen appropriately, then the magnitude of the ideal sensitivities will be smaller or equal to 1/2.

Using Eqs. (3.2.40) and (3.2.41), the non-ideal sensitivities can be calculated as follows:

$$S_{G_1}^{\omega_o} = S_{G_3}^{\omega_o} = S_{\alpha}^{\omega_o} = S_{\beta}^{\omega_o} = \frac{1}{2} \tag{3.3.7}$$

$$S_{C_2}^{\omega_o} = S_{C_4}^{\omega_o} = S_{R_1}^{\omega_o} = S_{R_3}^{\omega_o} = -\frac{1}{2} \tag{3.3.8}$$

$$S_{G_1}^{Q} = S_{R_3}^{Q} = S_{\alpha}^{Q} = S_{\beta}^{Q} = \frac{1}{2} \tag{3.3.9}$$

$$S^{Q}_{G_3} = S^{Q}_{R_1} = -\frac{1}{2} \tag{3.3.10}$$

$$S^{Q}_{C_2} = \frac{1}{2} - \frac{C_2}{C_2 + C_4} \tag{3.3.11}$$

$$S^{Q}_{C_4} = \frac{1}{2} - \frac{C_4}{C_2 + C_4}\,. \tag{3.3.12}$$

Again, if passive component values are chosen appropriately, then the magnitude of the sensitivities due to non-ideal effects will also be smaller or equal to1/2.

3.4 EXPERIMENTAL AND SIMULATION RESULTS

The validity of the proposed filter shown in Fig. 3.2 has been verified both experimentally and through PSPICE simulations. For experimental verification the AD844 IC manufactured by Analog Devices was used (Analog Devices, 1990). Since AD844 can realize only CCII+s, the CCII- had to be constructed from two positive-type second generation current conveyors (Svoboda et al., 1991). The circuit was supplied with symmetrical voltages of $\mathrm{V_{cc}} = 12\ \mathrm{V}$ and $\mathrm{V_{ee}} = -12\ \mathrm{V}$, respectively and was designed using the parameters shown in Table 3.1.

Table 3.1 Design parameters used for verifying the validity of the voltage mode MISO filter using a single negative type current conveyor.

3dB cutoff frequency (f_o) (kHz)	C_2 (nF)	C_4 (nF)	R_1 ($\mathrm{k\Omega}$)	R_3 ($\mathrm{k\Omega}$)
48.2	**1**	**1**	**3.3**	**3.3**

The simulations were carried out using the model parameters of AD844 from the built in library of PSPICE simulation program.

The simulation and experimental results for the second-order low-pass, high-pass, band-pass, and band-reject filters are shown in Fig. 3.8 through Fig. 3.11, respectively. Furthermore, Fig. 3.12 shows the filter responses for different configurations on a single graph for comparison. Although, the experimental and simulation results well fit into one another over a wide range of frequency, some discrepancies can be observed in the results. These discrepancies are related with the non-ideal characteristics of AD844 IC and the experimental equipment.

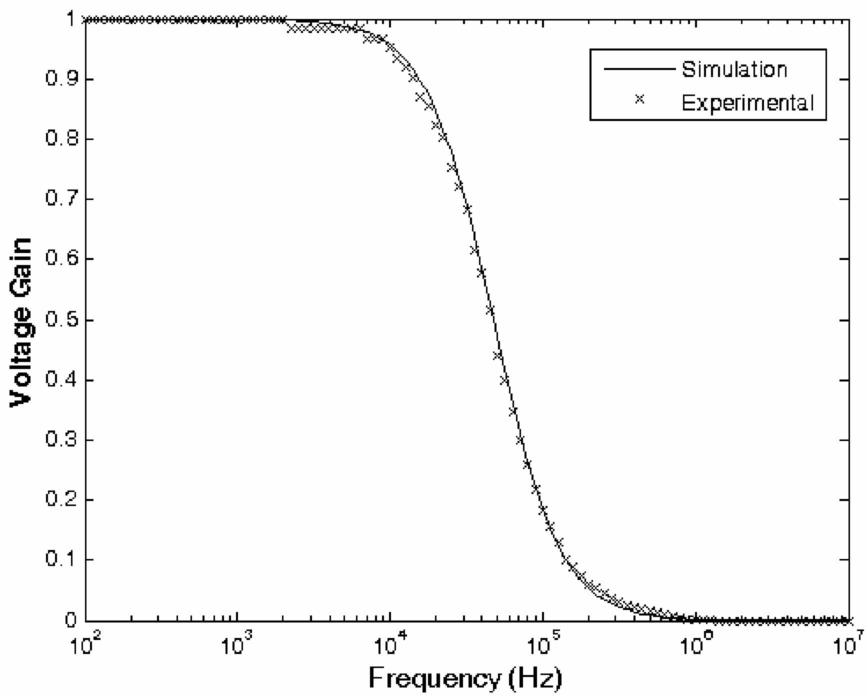

Figure 3.8 Simulation and experimental results for the proposed low-pass (LP) filter.

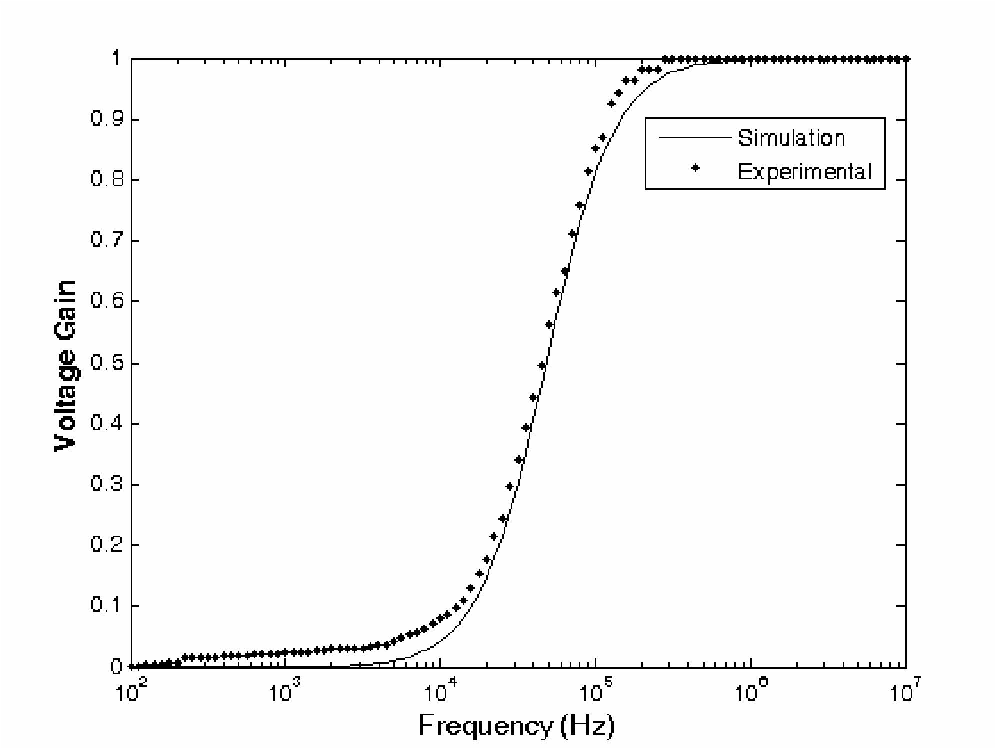

Figure 3.9 Simulation and experimental results for the proposed high-pass (HP) filter.

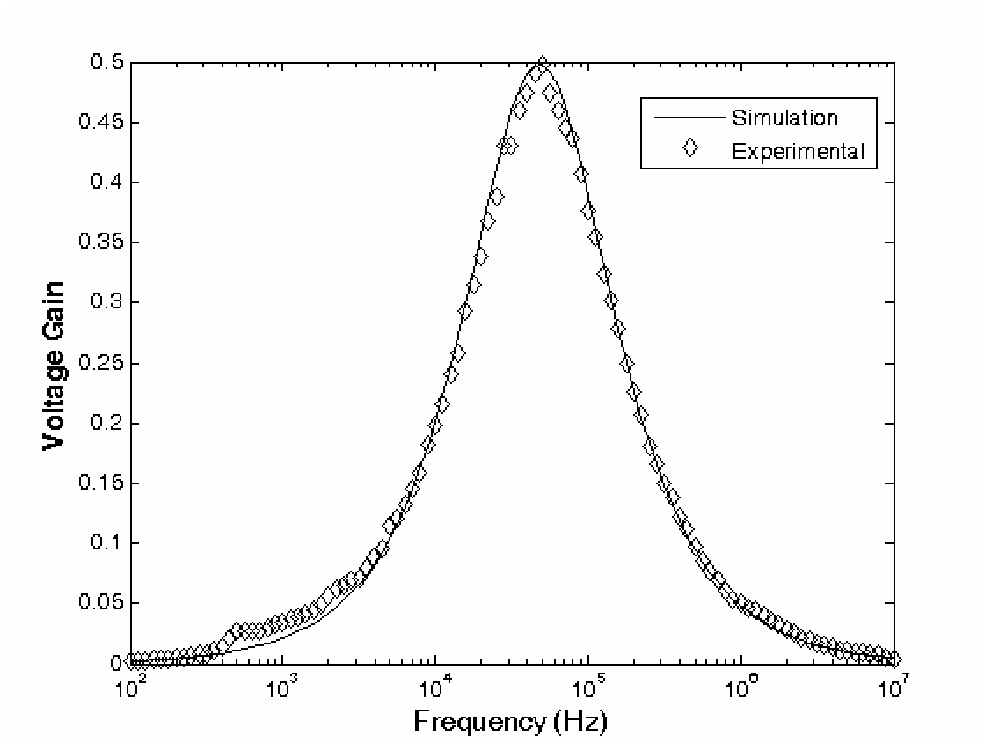

Figure 3.10 Simulation and experimental results for the proposed band-pass (BP) filter.

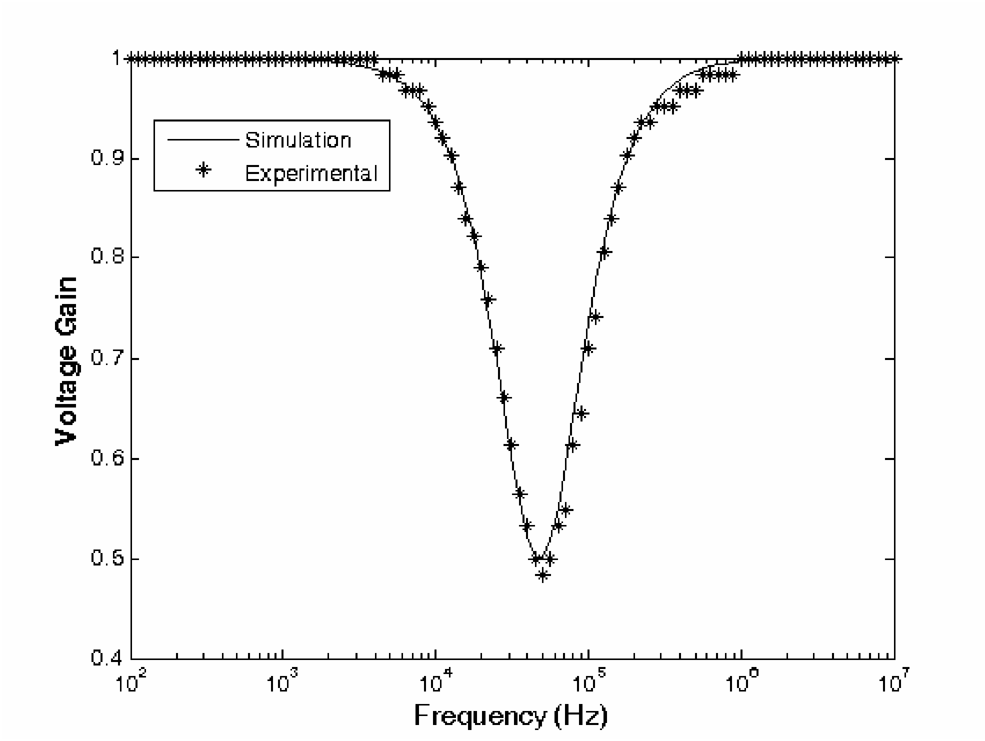

Figure 3.11 Simulation and experimental results for the proposed band-reject (BR) filter.

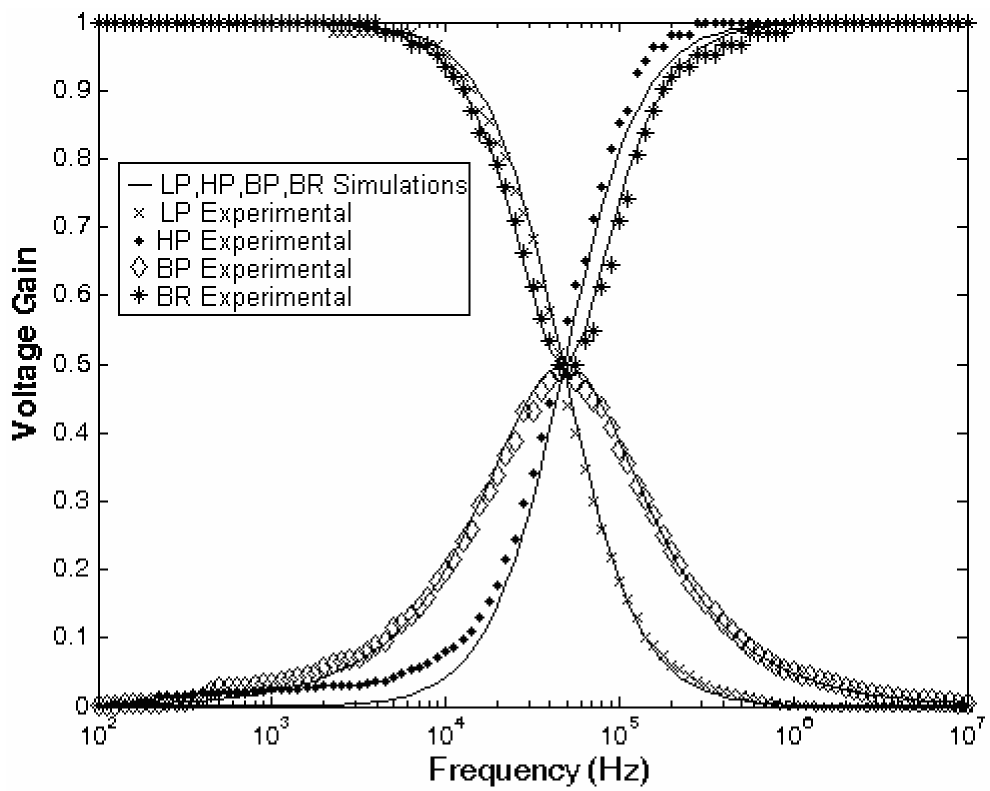

Figure 3.12 Comparison of simulation and experiment results for the proposed LP, HP, BP and BR filters.

CHAPTER 4

A VOLTAGE MODE MULTIPLE INPUT SINGLE OUTPUT (MISO) FILTER USING A SINGLE POSITIVE TYPE CURRENT CONVEYOR

4.1 INTRODUCTION

In this Chapter, the experimental verification of a voltage-mode multiple-input single-output multifunction filter using a single current conveyor proposed by Sagbas (Sagbas, 2003) is presented. The current conveyor is realized by a commercially available current feedback operational amplifier AD844 of Analog Devices. The experimental results are also compared with PSPICE simulations. Effect of the non-idealities and the sensitivity analysis of the proposed filter are also examined. The circuit uses one positive-type second generation current conveyor (CCII+), three resistors and two capacitors. The use of CCII+ simplifies the filter circuit configuration. This filter which possesses three-inputs and one-output can generate all biquadratic filtering functions of low-pass, high-pass, band-pass and band-reject at the output terminal by selecting different input signal combinations.

Recently, many MISO universal biquadratic filters using current conveyors or current conveyor based active elements have been reported in the literature. Some of these filters employ two CCII+s and one voltage follower (Chang and Tu., 1999), (Ozoguz and Gunes., 1996). Some other filters employ one CCII+, one negative type second generation current conveyor (CCII-), and two capacitors and three resistors (Horng et al., 1996), (Liu and Lee., 1997).

The multifunction filter proposed by Sagbas (Sagbas, 2003) has the following advantages:

(i) The use of current conveyor eliminates the disadvantage possessed by voltage-mode circuits using operational amplifiers. (Wilson et al., 1990), (Wandsworth et al., 1989).

(ii) Realization of all the basic filter functions: low-pass, high-pass, band-pass, band-reject, and all-pass.

(iii) Low passive and active sensitivities.

(iv) Undamped natural frequency is independent from the active parameters.

(v) Use of positive-type second generation current conveyor which is more suitable in IC manufacturing technology than negative-type second generation current conveyor.

(vi) Ability to adjust the natural frequency and the quality factor.

This chapter is divided into several sections. Section 4.2 presents circuit description and the analysis of the filter proposed by Sagbas (Sagbas, 2003) for both ideal and non-ideal cases. In section 4.3, the sensitivity analysis of the filter proposed by Sagbas (Sagbas, 2003) is presented. In section 4.4, the experimental and simulation results are presented.

4.2 CIRCUIT DESCRIPTION AND ANALYSIS OF THE MULTIFUNCTION FILTER

4.2.1 Ideal Case

The block diagram of a positive-type second generation current conveyor (CCII+) is shown in Fig. 4.1. The terminal equations for the ideal case can be written as (Smith et al., 1970),

$$I_y = 0 \tag{4.2.1}$$

$$V_x = V_y \tag{4.2.2}$$

$$I_z = I_x . \tag{4.2.3}$$

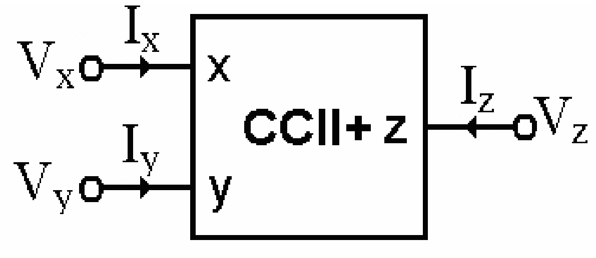

Figure 4.1 Block diagram of a positive type second generation current conveyor (CCII+).

The input impedances of the ideal CCII+ are infinite at terminal y and zero at terminal x, respectively. The terminal z is equivalent to a current generator possesses infinite output impedance.

The multifunction filter proposed by Sagbas (Sagbas, 2003) is shown in Fig. 4.2. The circuit employs only one CCII+ and five passive elements (two capacitors and three resistances). In order to analyze the proposed circuit shown in Fig. 4.2, we apply the relations given by Eqs. (4.2.1), through (4.2.3).

The current equations of the passive components can be written as

$$I_{R_1} = \frac{-V_z}{R_1} \tag{4.2.4}$$

$$I_{R_2} = \frac{V_1 - V_O}{R_2} \tag{4.2.5}$$

$$I_{R_3} = \frac{V_2 - V_O}{R_3} \tag{4.2.6}$$

$$I_{C_1} = sC_1(V_O - V_z) \tag{4.2.7}$$

$$I_{C_2} = sC_2(V_3 - V_z)\,. \tag{4.2.8}$$

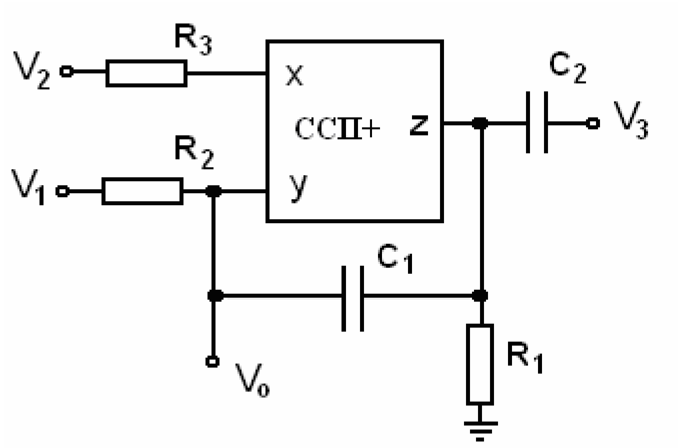

Figure 4.2 Circuit diagram of the voltage-mode multi-input single-output multifunction filter proposed by Sagbas (Sagbas, 2003).

Assuming that $I_{C_1} = I_{R_2}$, then Eq. (4.2.5) and Eq. (4.2.7) become

$$\frac{V_1 - V_O}{R_2} = sC_1(V_O - V_z)\,. \tag{4.2.9}$$

Eq. (4.2.9) can be simplified as

$$V_z = V_O - \frac{V_1 - V_O}{sC_1R_2}\,. \tag{4.2.10}$$

By writing a KCL equation at the output node of the circuit shown in Fig. 4.2, we obtain

$$I_z = I_{C_1} + I_{C_2} + I_{R_1}\,. \tag{4.2.11}$$

Assuming that $I_z = I_{R_3}$, then Eq. (4.2.11) becomes

$$I_{R_3} = I_{C_1} + I_{C_2} + I_{R_1}\,. \tag{4.2.12}$$

Substituting Eqs. (4.2.4), (4.2.6), (4.2.7) and (4.2.8) into Eq. (4.2.12) gives

$$\frac{V_2 - V_O}{R_3} = \frac{-V_z}{R_1} + sC_1(V_O - V_z) + sC_2(V_3 - V_z)\,. \tag{4.2.13}$$

Eq. (4.2.13) can be simplified as follows:

$$\frac{V_2 - V_O}{R_3} = sC_1V_O + sC_2V_3 + V_z(-\frac{1}{R_1} - sC_1 - sC_2)\,. \tag{4.2.14}$$

Substituting Eq. (4.2.10) into Eq. (4.2.14) gives

$$\frac{V_2 - V_O}{R_3} = sC_1V_O + sC_2V_3 + (V_O - \frac{V_1 - V_O}{sC_1R_2})(-\frac{1}{R_1} - sC_1 - sC_2)\,. \tag{4.2.15}$$

Rearranging the terms in Eq. (4.2.15) gives the transfer function of the filter proposed by Sagbas (Sagbas, 2003) as:

$$V_o(s) = \frac{s^2(R_1R_2R_3C_1C_2)V_3 + s(R_1R_3C_1V_1 + R_1R_3C_2V_1 - R_1R_2C_1V_2) + R_3V_1}{s^2R_1R_2R_3C_1C_2 + s(R_1R_3C_1 + R_1R_3C_2 - R_1R_2C_1 + R_2R_3C_1) + R_3}\,. \tag{4.2.16}$$

<u>Special Cases:</u>

(i) Low-pass (LP) filter realization:

In order to obtain a low-pass response from the multifunction filter proposed by Sagbas (Sagbas, 2003), the input signal is applied through the terminals V_1 and V_2 while the terminal V_3 is grounded and passive components are chosen as $C_1 = C_2$ and $R_2 = 2R_3$. Hence, the transfer function given by Eq. (4.2.16) becomes as:

$$V_o(s) = \frac{R_3}{s^2R_1R_2R_3C_1C_2 + s(R_2R_3C_1) + R_3}V_1\,. \tag{4.2.17}$$

The circuit diagram which gives a low-pass filter response is shown in Fig. 4.3.

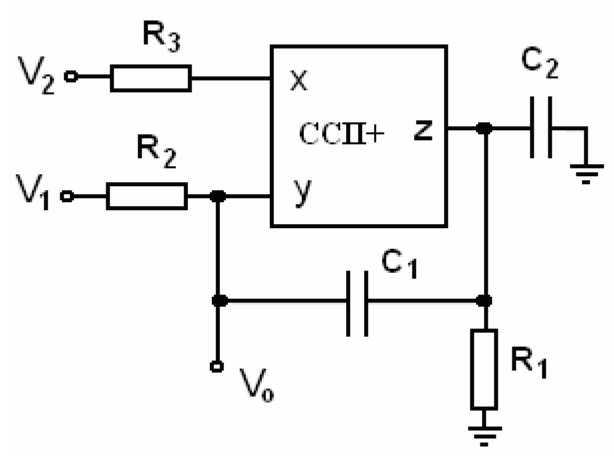

Figure 4.3 Circuit diagram of the filter showing low-pass filter configuration.

(ii) High-pass (HP) filter realization:

In order to obtain a high-pass response from the multifunction filter proposed by Sagbas (Sagbas, 2003), the input signal is applied through the terminal V_3 while the terminals V_1 and V_2 are grounded. Hence, the transfer function given by Eq. (4.2.16) becomes as:

$$V_o(s) = \frac{s^2(R_1R_2R_3C_1C_2)}{s^2R_1R_2R_3C_1C_2 + s(R_1R_3C_1 + R_1R_3C_2 - R_1R_2C_1 + R_2R_3C_1) + R_3} V_3 . \quad (4.2.18)$$

The circuit diagram which gives a high-pass filter response is shown in Fig. 4.4.

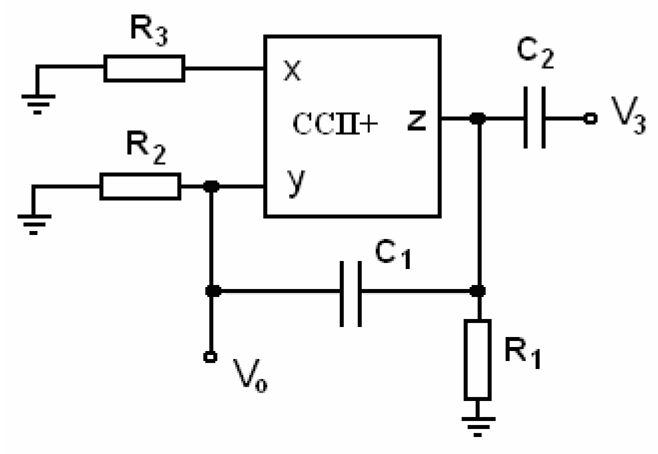

Figure 4.4 Circuit diagram of the filter showing high-pass filter configuration.

(iii) Band-pass (BP) filter realization:

In order to obtain a band-pass response from the multifunction filter proposed by Sagbas (Sagbas, 2003), the input signal is applied through the terminal V_2 while the terminals V_1 and V_3 are grounded. Hence, the transfer function given by Eq. (4.2.16) becomes as:

$$V_o(s) = \frac{-R_1R_2C_1}{s^2R_1R_2R_3C_1C_2 + s(R_1R_3C_1 + R_1R_3C_2 - R_1R_2C_1 + R_2R_3C_1) + R_3} V_2 . \tag{4.2.19}$$

The circuit diagram which gives a band-pass filter response is shown in Fig. 4.5.

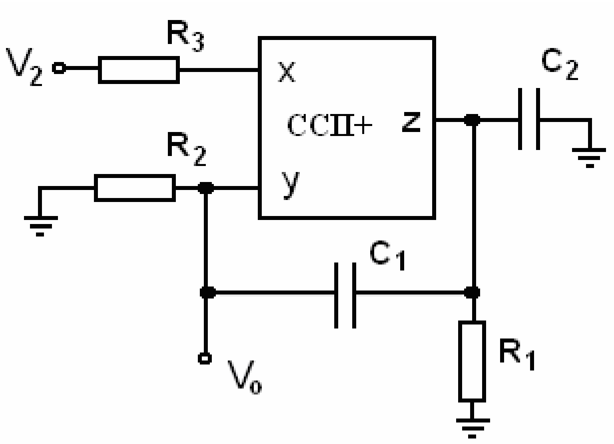

Figure 4.5 Circuit diagram of the filter showing band-pass filter configuration.

(iv) Band-reject (BR) filter realization:

In order to obtain a band-reject response from the multifunction filter proposed by Sagbas (Sagbas, 2003), the input signal is applied through the terminals V_1, V_2 and V_3 and the passive components are chosen as $C_1 = C_2$ and $R_2 = 2R_3$. Hence, the transfer function given by Eq. (4.2.16) becomes as:

$$V_o(s) = \frac{s^2(R_1R_2R_3C_1C_2) + R_3}{s^2R_1R_2R_3C_1C_2 + s(R_1R_3C_1 + R_1R_3C_2 - R_1R_2C_1 + R_2R_3C_1) + R_3} V_1 . \tag{4.2.20}$$

The circuit diagram which gives a band-reject filter response is shown in Fig. 4.6.

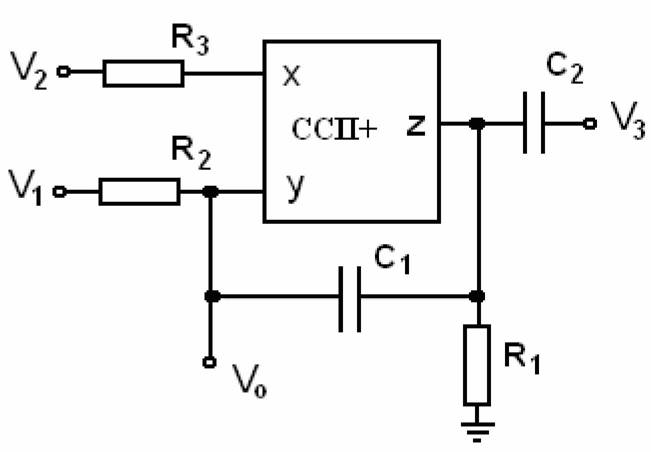

Figure 4.6 Circuit diagram of the filter showing band-reject filter configuration.

(v) All-pass (AP) filter realization:

In order to obtain an all-pass response from the multifunction filter proposed by Sagbas (Sagbas, 2003), the input signal is applied through the terminals V_1, V_2 and V_3. Choosing $V_1 = V_3 = V_2/2$ and the passive components as $R_1 = R_3 = R_2/2$, and $C_1 = C_2$ gives the all-pass filter response. Hence, the transfer function given by Eq. (4.2.16) becomes as:

$$V_o(s) = \frac{s^2(R_1R_2R_3C_1C_2) - s(2R_1R_3C_1) + R_3}{s^2(R_1R_2R_3C_1C_2) + s(2R_1R_3C_1) + R_3} V_1 . \quad (4.2.21)$$

The circuit diagram which gives an all-pass filter response is shown in Fig. 4.7.

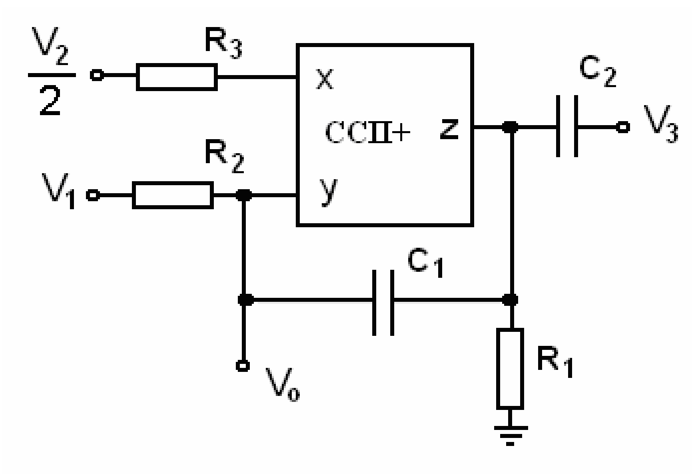

Figure 4.7 Circuit diagram of the filter showing all-pass filter configuration.

From the above analysis, it can be observed that all the standard filter functions namely; high-pass, band-pass, low-pass, band-reject and all-pass can be obtained from the filter proposed by Sagbas (Sagbas, 2003). Furthermore, in order to obtain the same natural frequency and quality factor for all filter characteristics, the same constraints for passive component must be chosen.

The natural frequency and the quality factor of the circuit proposed by Sagbas (Sagbas, 2003) are obtained from the denominator of the transfer function given by Eq. (4.2.16) as:

$$\omega_o = \frac{1}{\sqrt{R_1 R_2 C_1 C_2}} \tag{4.2.22}$$

$$Q = \frac{R_3 \sqrt{R_1 R_2 C_1 C_2}}{R_1 R_3 (C_1 + C_2) + (R_3 - R_1) R_2 C_1}. \tag{4.2.23}$$

4.2.2 Non-ideal Case

Taking the non-idealities into account, the terminal equations of the CCII+ shown in Fig. 4.1 can be written as

$$I_y = 0 \tag{4.2.24}$$

$$V_x = \beta V_y \tag{4.2.25}$$

$$I_z = -\alpha I_x \tag{4.2.26}$$

where, $\beta = 1 - \varepsilon_V$ and $\alpha = 1 - \varepsilon_i$. ε_V $(|\varepsilon_V| << 1)$ and ε_i $(|\varepsilon_i| << 1)$ denote the voltage and current tracking errors, respectively (Smith et al., 1970).

The currents through each passive element shown in Fig. 4.2 can be written as

$$I_{R_1} = \frac{-V_z}{R_1} \tag{4.2.27}$$

$$I_{R_2} = \frac{V_1 - V_x}{R_2} \tag{4.2.28}$$

$$I_{R_3} = \frac{V_2 - V_O}{R_3} \tag{4.2.29}$$

$$I_{C_1} = sC_1(V_O - V_z) \tag{4.2.30}$$

$$I_{C_2} = sC_2(V_3 - V_z)\,. \tag{4.2.31}$$

From Fig. 4.2, it can be seen that $I_{C_1} = I_{R_2}$. Therefore, substituting Eq. (4.2.28) into Eq. (4.2.30) gives

$$\frac{V_1 - V_x}{R_2} = sC_1(V_O - V_z)\,. \tag{4.2.32}$$

Eq. (4.2.32) can be simplified as

$$V_z = V_O - \frac{V_1 - V_x}{sC_1 R_2}\,. \tag{4.2.33}$$

Substituting $V_x = \beta V_y = \beta V_O$, into Eq. (4.2.33) gives

$$V_z = V_O - \frac{V_1 - \beta V_O}{sC_1 R_2}\,. \tag{4.2.34}$$

By writing a KCL equation at the output node of the circuit shown in Fig. 4.2, we obtain

$$I_z = I_{C_1} + I_{C_2} + I_{R_1} \tag{4.2.35}$$

From Fig. 4.2, it is obvious that $I_z = I_{R_3}$. Therefore Eq. (4.2.35) becomes

$$I_{R_3} = I_{C_1} + I_{C_2} + I_{R_1} . \tag{4.2.36}$$

Substituting Eqs. (4.2.27), (4.2.29), (4.2.30) and (4.2.31) into Eq. (4.2.36) gives

$$\frac{V_2 - V_O}{R_3} = \frac{-V_z}{R_1} + sC_1(V_O - V_z) + sC_2(V_3 - V_z) . \tag{4.2.37}$$

Simplifying Eq. (4.2.37) gives

$$\frac{V_2 - V_O}{R_3} = sC_1V_O + sC_2V_3 + V_z(-\frac{1}{R_1} - sC_1 - sC_2) . \tag{4.2.38}$$

Substituting Eq. (4.2.34) into Eq. (4.2.38) gives

$$\frac{V_2 - V_O}{R_3} = sC_1V_O + sC_2V_3 + (V_O - \frac{V_1 - \beta V_O}{sC_1R_2})(-\frac{1}{R_1} - sC_1 - sC_2) .. \tag{4.2.39}$$

After rearranging the terms in Eq. (4.2.39), the denominator polynomial of the transfer functions for the multifunction filter proposed by Sagbas (Sagbas, 2003) becomes

$$D(s) = s^2 R_1 R_2 R_3 C_1 C_2 + s\left[R_1 R_3 (C_1 + C_2) + R_2 C_1 (R_3 - \alpha\beta R_1)\right] + R_3 \tag{4.2.40}$$

Using Eq. (4.2.40), the natural frequency and the quality factor for the non-ideal case can be calculated as

$$\omega_o = \frac{1}{\sqrt{R_1 R_2 C_1 C_2}} \tag{4.2.41}$$

$$Q = \frac{R_3 \sqrt{R_1 R_2 C_1 C_2}}{R_1 R_3 (C_1 + C_2) + (R_3 - \alpha\beta R_1) R_2 C_1} . \tag{4.2.42}$$

From Eq. (4.2.41), it can be observed that the undamped natural frequency is independent from the active parameters α and β.

4.3 SENSITIVITY ANALYSIS

The ideal sensitivities of the natural frequency and the quality factor with respect to passive components are calculated using Eqs. (4.2.22) and (4.2.23) as follows;

$$S_{R_1}^{\omega_o} = S_{R_2}^{\omega_o} = S_{C_1}^{\omega_o} = S_{C_2}^{\omega_o} = -\frac{1}{2} \tag{4.3.1}$$

$$S_{R_3}^{\omega_o} = 0 \tag{4.3.2}$$

$$S_{R_1}^{Q} = \frac{1}{2} - R_1 \frac{R_3(C_1 + C_2) - R_2 C_1}{p_1} \tag{4.3.3}$$

$$S_{R_2}^{Q} = \frac{1}{2} - R_2 \frac{C_1(R_3 - R_1)}{p_1} \tag{4.3.4}$$

$$S_{R_3}^{Q} = \frac{1}{2} - R_3 \frac{R_1(C_1 + C_2) + R_2 C_1}{p_1} \tag{4.3.5}$$

$$S_{C_1}^{Q} = \frac{1}{2} - C_1 \frac{R_1 R_3 + R_2(R_1 - R_3)}{p_1} \tag{4.3.6}$$

$$S_{C_2}^{Q} = \frac{1}{2} - C_2 \frac{R_1 R_3}{p_1} \tag{4.3.7}$$

where,

$$p_1 = R_1 R_3 (C_1 + C_2) + (R_3 - R_1) R_2 C_1 \ . \tag{4.3.8}$$

If the passive component values are chosen appropriately, then the magnitude of the ideal sensitivities will be smaller than 1/2. Otherwise, the sensitivities can be become infinity as in oscillator applications.

Using Eqs. (4.2.41) and (4.2.42), the non-ideal sensitivities can be found as

$$S_{R_1}^{\omega_o} = S_{R_2}^{\omega_o} = S_{C_1}^{\omega_o} = S_{C_2}^{\omega_o} = -\frac{1}{2} \tag{4.3.9}$$

$$S_{R_3}^{\omega_o} = 0 \tag{4.3.10}$$

$$S_{R_1}^{Q} = \frac{1}{2} - R_1 \frac{R_3(C_1 + C_2) - \alpha\beta R_2 C_1}{p_2} \tag{4.3.11}$$

$$S_{R_2}^{Q} = \frac{1}{2} - R_2 \frac{C_1(R_3 - \alpha\beta R_1)}{p_2} \tag{4.3.12}$$

$$S_{R_3}^{Q} = \frac{1}{2} - R_3 \frac{R_1(C_1 + C_2) + R_2 C_1}{p_2} \tag{4.3.13}$$

$$S_{C_1}^{Q} = \frac{1}{2} - C_1 \frac{R_1 R_3 + R_2(R_1 - \alpha\beta R_3)}{p_2} \tag{4.3.14}$$

$$S_{C_2}^{Q} = \frac{1}{2} - C_2 \frac{R_1 R_3}{p_2} \tag{4.3.15}$$

where,

$$p_2 = R_1 R_3 (C_1 + C_2) + (R_3 - \alpha\beta R_1) R_2 C_1 \,. \tag{4.3.16}$$

Again, if passive component values are chosen appropriately, then the magnitude of the sensitivities due to non-ideal effects will also be small than 1/2. Otherwise, the sensitivities can be become infinity as in oscillator applications.

4.4 EXPERIMENTAL AND SIMULATION RESULTS

The validity of the filter proposed by Sagbas (Sagbas, 2003) shown in Fig. 4.2 has been verified both experimentally and through PSPICE simulations. For experimental verification, the AD844 IC manufactured by Analog Devices was used (Analog Devices, 1990). The circuit was supplied with symmetrical voltages of $V_{cc} = 12$ V and $V_{ee} = -12$ V, respectively and was designed using the parameters shown in Table 4.1.

Table 4.1 Design parameters used for verifying the validity of the voltage mode MISO filter using a single positive type current conveyor.

3dB cutoff frequency (f_O) (kHz)	C_1 (nF)	C_2 (nF)	R_1 (kΩ)	R_2 (kΩ)	R_3 (kΩ)
112.5	**1**	**1**	**1**	**2**	**1**

The simulations were carried out using the model parameters of AD844 from the built in library of PSPICE simulation program.

The simulation and experimental results for the second-order low-pass, high-pass, and band-pass filters are shown in Fig. 4.8 through Fig. 4.10, respectively. Furthermore, Fig. 4.11 shows the filter responses for different configurations on a single graph for comparison. Although, the experimental and simulation results well fit into one another over a wide range of frequency, some discrepancies can be observed in the results. These discrepancies are related with the non-ideal characteristics of AD844 IC and the experimental equipment.

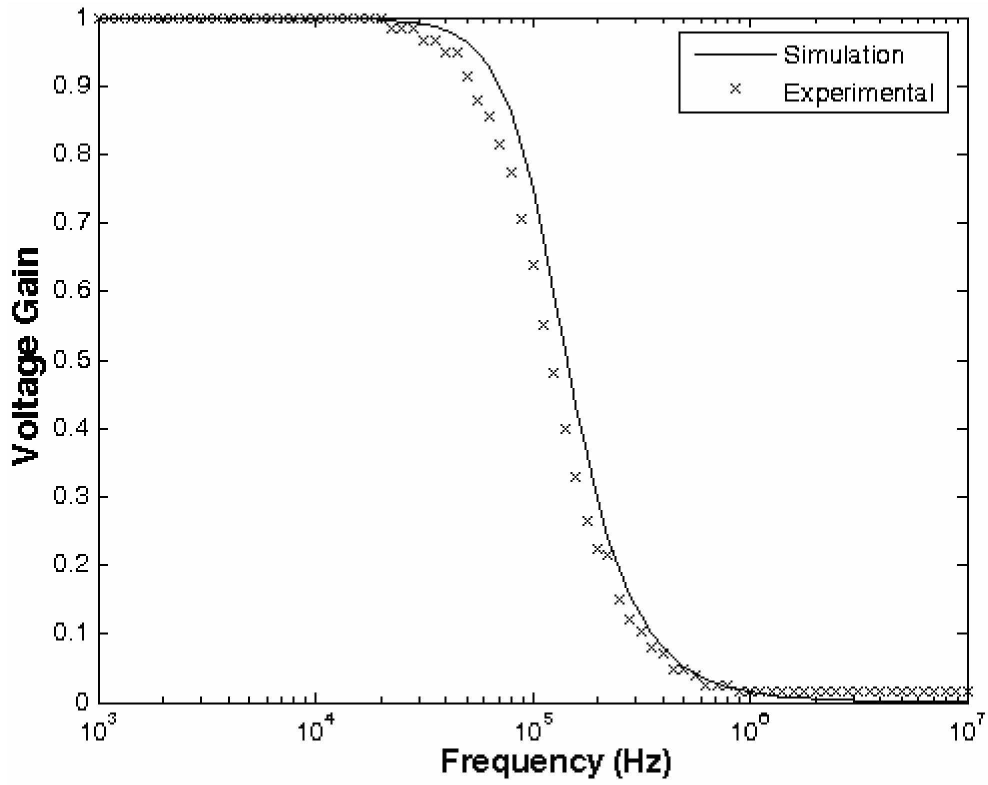

Figure 4.8 Simulation and experimental results for the low-pass (LP) filter proposed by Sagbas (Sagbas, 2003).

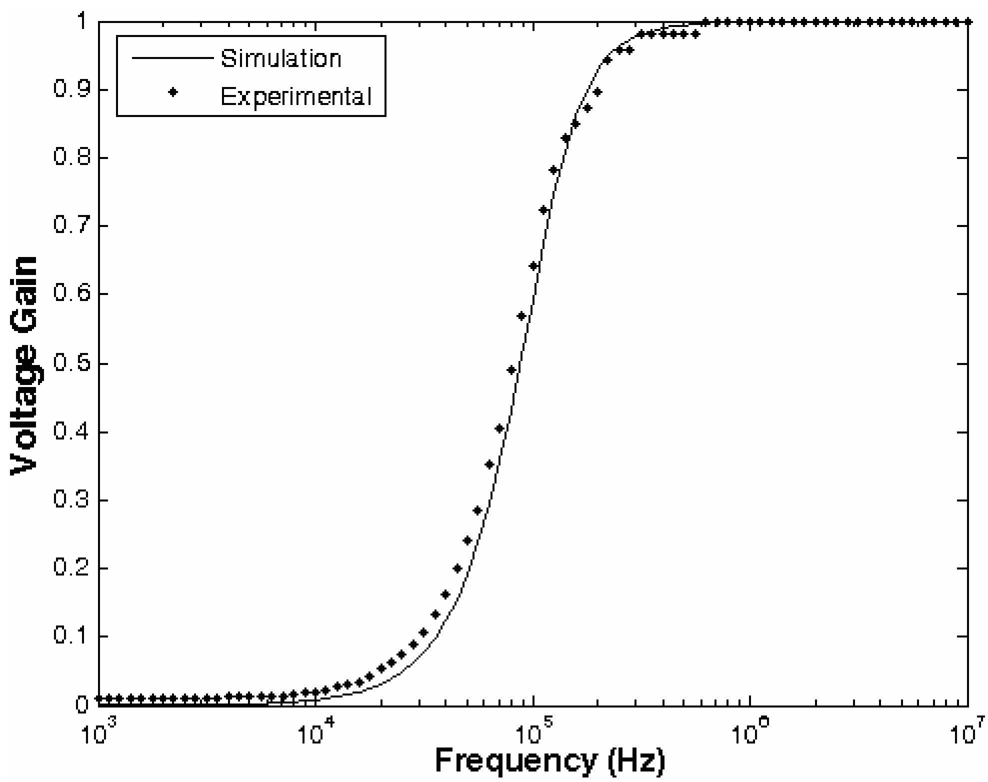

Figure 4.9 Simulation and experimental results for the high-pass (HP) filter proposed by Sagbas (Sagbas, 2003).

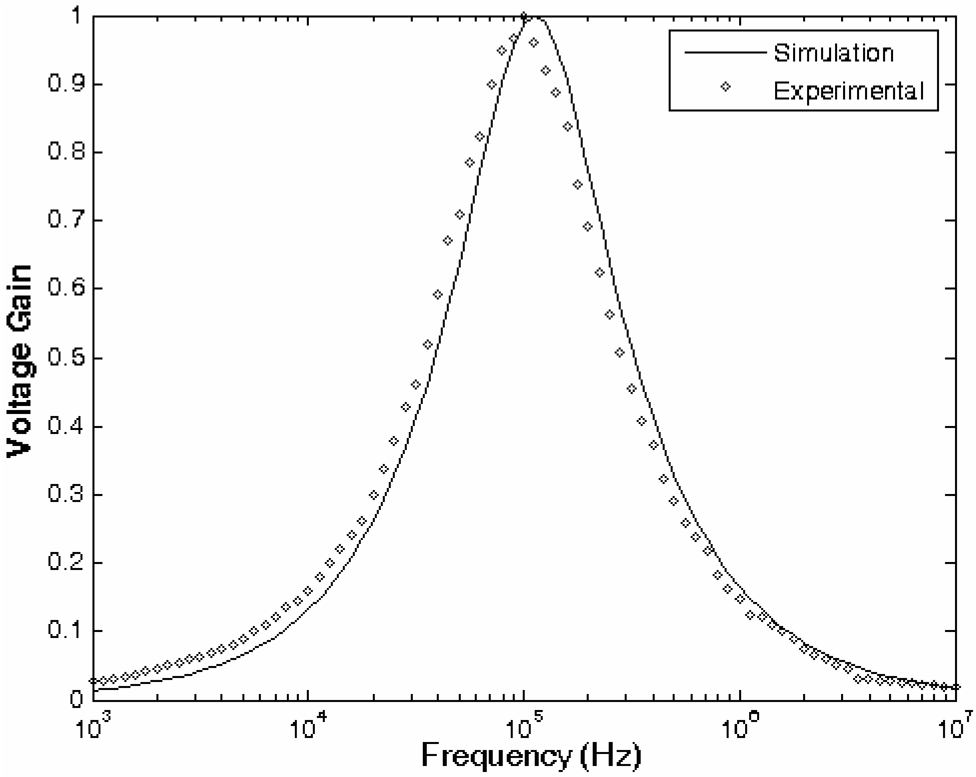

Figure 4.10 Simulation and experimental results for the band-pass (BP) filter proposed by Sagbas (Sagbas, 2003).

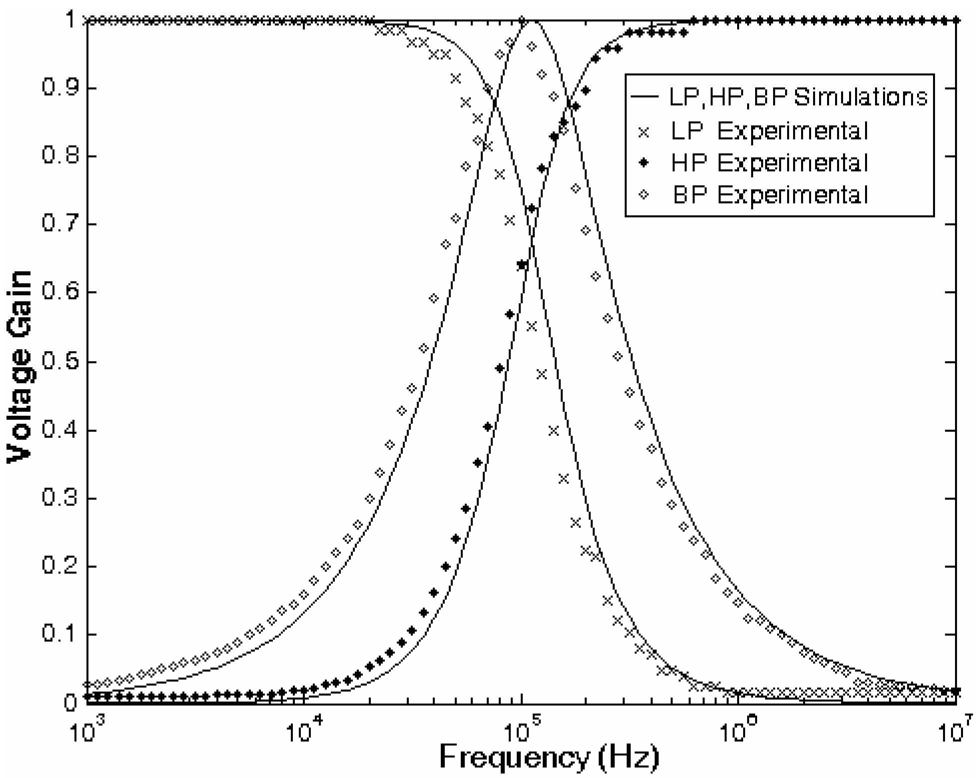

Figure 4.11 Comparison of simulation and experimental results for the LP, HP, and BP filters proposed by Sagbas (Sagbas, 2003).

CHAPTER 5

A VOLTAGE MODE MULTIPLE INPUT SINGLE OUTPUT (MISO) FILTER USING TWO CURRENT CONVEYORS

5.1 INTRODUCTION

In this chapter, the experimental verification of a voltage-mode multiple-input single-output multifunction filter using two current conveyors proposed by Sagbas et al. (Sagbas et al., 2005) is presented. The current conveyors are realized by a commercially available current feedback operational amplifier AD844 of Analog Devices. The experimental results are also compared with PSPICE simulations. Effect of the non-idealities and the sensitivity analysis of the proposed filter are also examined. The circuit uses one positive-type second generation current conveyor (CCII+), one negative-type second generation current conveyor (CCII-), three resistors, and two capacitors. This filter which possesses three-inputs and one-output can generate all biquadratic filtering functions of low-pass, high-pass, band-pass and band-reject at the output terminal by selecting different input signal combinations.

The multifunction filter proposed by Sagbas et al. (Sagbas et al., 2005) has the following advantages:

(i) Voltage-mode circuits using conventional operational amplifier have the disadvantage of severely reduced bandwidth at higher gains, because of the op-amp's fixed gain-bandwidth product. These disadvantages can be eliminated by using current conveyors and current conveyor based active elements (Wilson et al., 1990), (Wandsworth et al., 1990).

(ii) Realization of all the basic filter functions: low-pass, high-pass, band-pass and band-reject.

(iii) Low passive and active sensitivities.

(iv) Ability to adjust the natural frequency and the quality factor.

This chapter is divided into several sections. Section 5.2 presents circuit description and the analysis of the multifunction filter proposed by Sagbas et al. (Sagbas et al., 2005) for both ideal and non-ideal cases. In section 5.3, the sensitivity analysis of the filter proposed by Sagbas et al. (Sagbas et al., 2005) is presented. In section 5.4, the experimental and simulation results are presented.

5.2 CIRCUIT DESCRIPTION AND ANALYSIS OF THE MULTIFUNCTION FILTER

5.2.1 Ideal Case

The block diagram of a second generation current conveyor (CCII) is shown in Fig. 5.1. The terminal equations for the ideal case can be written as (Smith et al., 1970). The multifunction filter proposed by Sagbas et al. is shown in Fig. 5.2 (Sagbas et al., 2005). The circuit employs one CCII+, one CCII-, and five passive elements (two capacitors and three resistances).

$$I_y = 0 \qquad (5.2.1)$$

$$V_x = V_y \qquad (5.2.2)$$

$$I_z = \pm I_x . \qquad (5.2.3)$$

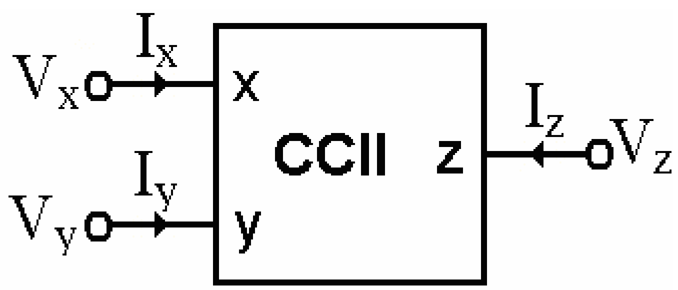

Figure 5.1 Block diagram of a second generation current conveyor (CCII).

The input impedances of the ideal CCII± are infinite at terminal *y* and zero at terminal *x*, respectively. The terminal *z*, which is equivalent to a current generator, possesses infinite output impedance.

The multifunction filter proposed by Sagbas et al. is shown in Fig. 5.2 (Sagbas et al., 2005). The circuit employs one CCII+, one CCII-, and five passive elements (two capacitors and three resistances). In order to analyze the proposed circuit shown in Fig. 5.2, we apply the relations given by Eqs. (5.2.1), through (5.2.3). Hence we obtain the following equations;

$$I_{y1} = I_{y2} = 0 \tag{5.2.4}$$

$$I_{z1} = -I_{x1} \tag{5.2.5}$$

$$I_{z2} = I_{x2} \tag{5.2.6}$$

$$V_{x1} = V_{y1} = V_O \tag{5.2.7}$$

$$V_{x2} = V_{y2}\,. \tag{5.2.8}$$

The current equations of the passive components can be written as

$$I_{R_1} = \frac{V_2 - V_{y1}}{R_1} \tag{5.2.9}$$

$$I_{R_2} = \frac{V_3 - V_{x1}}{R_2} \tag{5.2.10}$$

$$I_{R_3} = -\frac{V_{x2}}{R_3} \tag{5.2.11}$$

$$I_{C_1} = sC_1(V_1 - V_{y1}) \tag{5.2.12}$$

$$I_{C_2} = sC_2(V_{y2})\,. \tag{5.2.13}$$

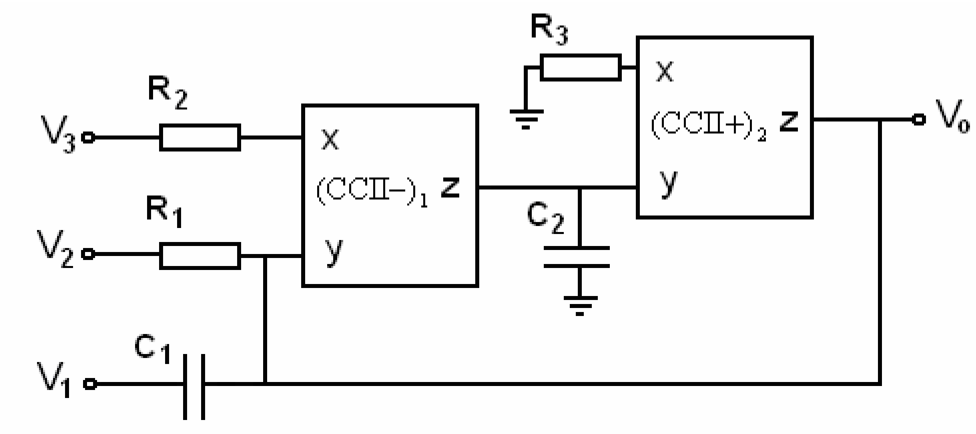

Figure 5.2 Circuit diagram of the voltage-mode multi-input single-output multifunction filter using two current conveyors proposed by Sagbas et al. (Sagbas et al., 2005).

The input currents in Fig. 5.2 are related with each other by the following equations:

$$I_{z2} = I_{x2} = I_{R_3} \tag{5.2.14}$$

$$I_{z1} = -I_{x1} = -I_{R_2} = -I_{C_2}\,. \tag{5.2.15}$$

Substituting Eq. (5.2.6) and (5.2.7) into Eq. (5.2.9) through Eq. (5.2.12), we obtain

$$I_{R_1} = \frac{V_2 - V_O}{R_1} \tag{5.2.16}$$

$$I_{R_2} = \frac{V_3 - V_O}{R_2} \tag{5.2.17}$$

$$I_{R_3} = I_{x2} = -\frac{V_{x2}}{R_3} \tag{5.2.18}$$

$$I_{C_1} = sC_1(V_1 - V_O)\,. \tag{5.2.19}$$

By writing a KCL equation at the input node of the circuit shown in Fig. 5.2, we obtain

$$I_{C_1} + I_{R_1} = I_{y1} + I_{z2}\,. \tag{5.2.20}$$

Substituting Eqs. (5.2.4), (5.2.16), and (5.2.19) into Eq. (5.2.20) results

$$-\frac{V_{x2}}{R_3} = sC_1(V_1 - V_O) + \frac{V_2 - V_O}{R_1}\,. \tag{5.2.21}$$

Eq. (5.2.21) can be simplified as

$$V_{x2} = -sC_1R_3(V_1 - V_O) - R_3\frac{V_2 - V_O}{R_1} \ . \tag{5.2.22}$$

Substituting Eqs. (5.2.13) and (5.2.17) into Eq. (5.2.15) gives

$$V_{y2} = \frac{V_3 - V_O}{sC_2R_2} \ . \tag{5.2.23}$$

From Eq. (5.2.8) $V_{x2} = V_{y2}$. Hence Eqs. (5.2.22) and (5.2.23) can be written as

$$\frac{V_3 - V_O}{sC_2R_2} = -sC_1R_3(V_1 - V_O) - R_3\frac{V_2 - V_O}{R_1} \ . \tag{5.2.24}$$

After rearranging the terms in the above equation, the transfer function of this circuit is found as

$$V_o = \frac{s^2R_1R_2R_3C_1C_2V_1 + sR_2R_3C_2V_2 + R_1V_3}{s^2R_1R_2R_3C_1C_2 + sR_2R_3C_2 + R_1} \ . \tag{5.2.25}$$

<u>Special Cases:</u>

(i) Low-pass (LP) filter realization:

In order to obtain a low-pass response from the multifunction filter proposed by Sagbas et al. (Sagbas et al., 2005), the input signal is applied through the terminal V_3 while the terminals V_1 and V_2 are grounded. Hence, the transfer function given by Eq. (5.2.25) becomes as follows:

$$V_o = \frac{R_1}{s^2R_1R_2R_3C_1C_2 + sR_2R_3C_2 + R_1}V_3 \ . \tag{5.2.26}$$

The circuit diagram which gives a low-pass filter response is shown in Fig. 5.3.

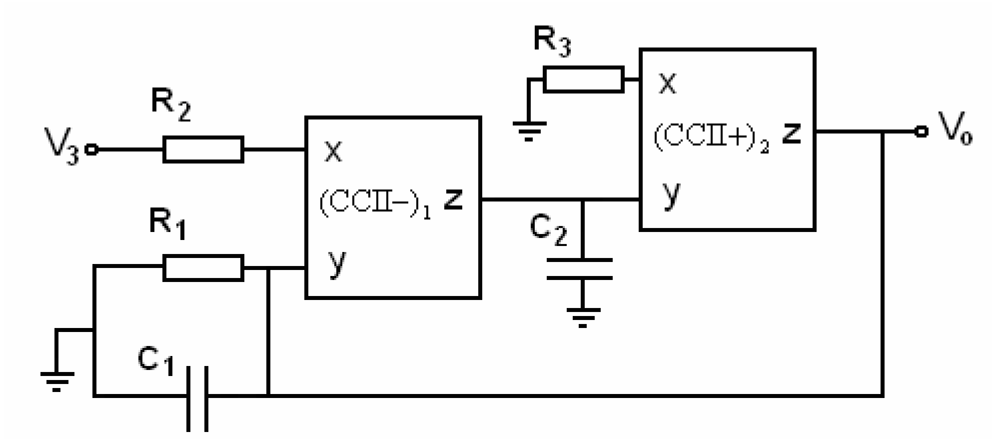

Figure 5.3 Circuit diagram of the filter showing low-pass filter configuration.

(ii) High-pass (HP) filter realization:

In order to obtain a high-pass response from the multifunction filter proposed by Sagbas et al. (Sagbas et al., 2005), the input signal is applied through the terminal V_1 while the terminals V_2 and V_3 are grounded. Hence, the transfer function given by Eq. (5.2.25) becomes as follows:

$$V_o = \frac{s^2 R_1 R_2 R_3 C_1 C_2}{s^2 R_1 R_2 R_3 C_1 C_2 + s R_2 R_3 C_2 + R_1} V_1 . \qquad (5.2.27)$$

The circuit diagram which gives a high-pass filter response is shown in Fig. 5.4.

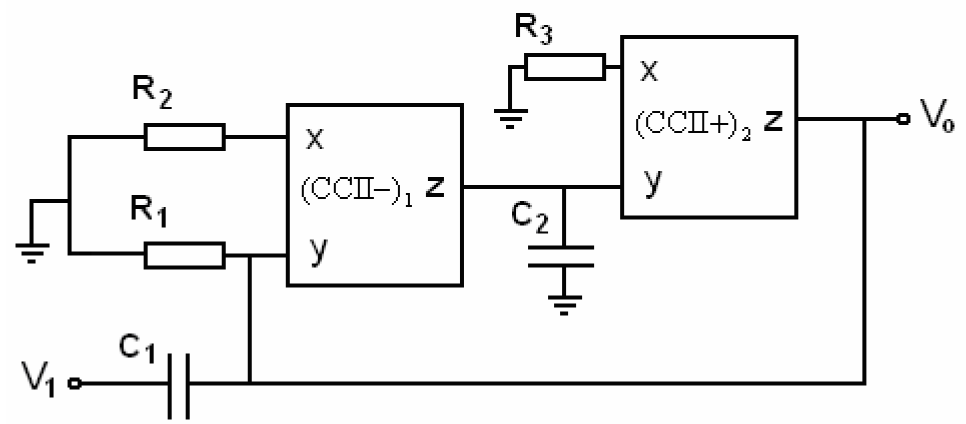

Figure 5.4 Circuit diagram of the filter showing high-pass filter configuration.

(iii) Band-pass (BP) filter realization:

In order to obtain a band-pass response from the multifunction filter proposed by Sagbas et al. (Sagbas et al., 2005), the input signal is applied through the terminal V_2 while the terminals V_1 and V_3 are grounded. Hence, the transfer function given by Eq. (5.2.25) becomes as follows:

$$V_o = \frac{sR_2R_3C_2}{s^2R_1R_2R_3C_1C_2 + sR_2R_3C_2 + R_1}V_2 . \quad (5.2.28)$$

The circuit diagram which gives a band-pass filter response is shown in Fig. 5.5.

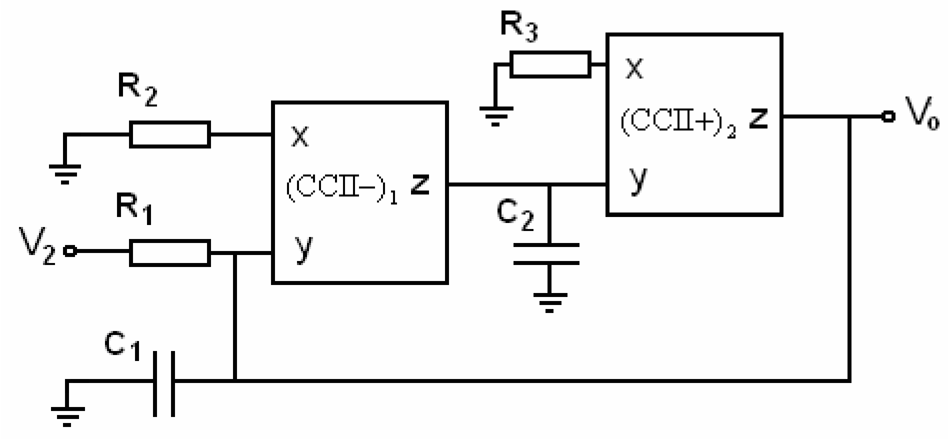

Figure 5.5 Circuit diagram of the filter showing band-pass filter configuration.

(iv) Band-reject (BR) filter realization:

In order to obtain a band-reject response from the multifunction filter proposed by Sagbas et al. (Sagbas et al., 2005), the input signal is applied through the terminals V_1 and V_3 while the terminal V_2 is grounded. Hence, the transfer function given by Eq. (5.2.25) becomes as follows:

$$V_o = \frac{s^2R_1R_2R_3C_1C_2 + R_1}{s^2R_1R_2R_3C_1C_2 + sR_2R_3C_2 + R_1}V_1 . \quad (5.2.29)$$

The circuit diagram which gives a band-reject filter response is shown in Fig. 5.6.

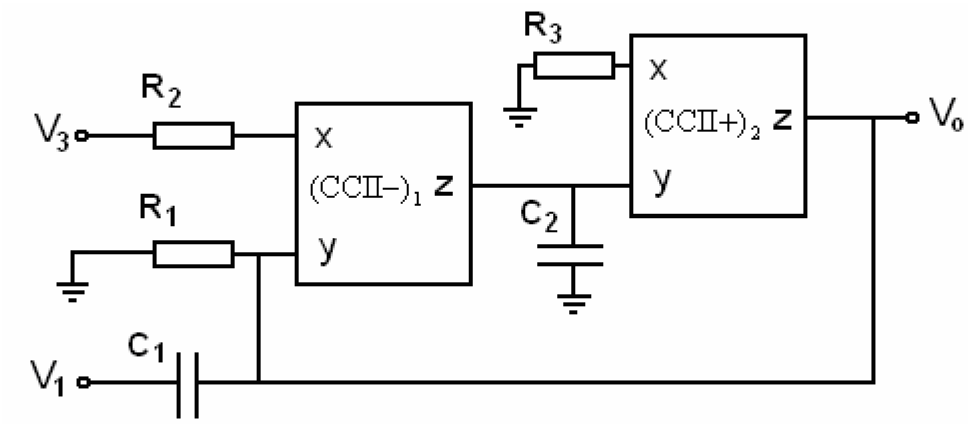

Figure 5.6 Circuit diagram of the filter showing band-reject filter configuration.

(v) All-pass (AP) filter realization:

In order to obtain an all-pass response from the multifunction filter proposed by Sagbas et al. (Sagbas et al., 2005), the input signal is applied through the terminals V_1, V_2 and V_3. Choosing $V_1 = -V_2 = V_3$ gives the all-pass filter response. Hence, the transfer function given by Eq. (5.2.25) becomes as follows:

$$V_o = \frac{s^2 R_1 R_2 R_3 C_1 C_2 - sR_2 R_3 C_2 + R_1}{s^2 R_1 R_2 R_3 C_1 C_2 + sR_2 R_3 C_2 + R_1} V_1 . \qquad (5.2.30)$$

The circuit diagram which gives an all-pass filter response is shown in Fig. 5.7.

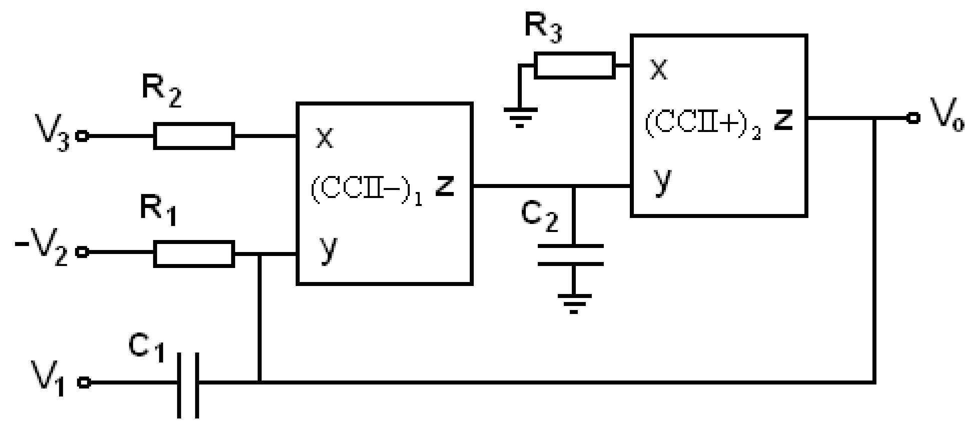

Figure 5.7 Circuit diagram of the filter showing all-pass filter configuration.

From the above analysis, it can be observed that all the standard filter functions, namely; high-pass, band-pass, low-pass, band-reject and all-pass can be obtained from the filter proposed by Sagbas et al. (Sagbas et al., 2005). It is also seen that the filter configurations do not require any inverting-type voltage input signals for realizing any second-order filter characteristics. Furthermore, in order to obtain the same natural frequency and quality factor for all filter characteristics, the same constraints for passive component must be chosen.

The natural frequency and the quality factor of the multifunction filter proposed by Sagbas et al. (Sagbas et al., 2005) are obtained from the denominator of the transfer function given by Eq. (5.2.25) as follows:

$$\omega_o = \frac{1}{\sqrt{R_2 R_3 C_1 C_2}} \tag{5.2.31}$$

$$Q = \sqrt{\frac{C_1}{C_2 R_2 R_3}} R_1 . \tag{5.2.32}$$

5.2.2 Non-ideal Case

Taking the non-idealities of the CCII into account, the terminal equations of the CCII shown in Fig. 5.1 can be written as

$$I_y = 0 \tag{5.2.33}$$

$$V_x = \beta V_y \tag{5.2.34}$$

$$I_z = \mp \alpha I_x . \tag{5.2.35}$$

where, $\beta = 1 - \varepsilon_V$ and $\alpha = 1 - \varepsilon_i$. ε_V ($|\varepsilon_V| << 1$) and ε_i ($|\varepsilon_i| << 1$) denote the voltage and current tracking errors, respectively (Smith et al., 1970).

The currents through each passive element shown in Fig. 5.2 can be written as

$$I_{y1} = I_{y2} = 0 \tag{5.2.36}$$

$$I_{z1} = -\alpha_1 I_{x1} \tag{5.2.37}$$

$$I_{z2} = \alpha_2 I_{x2} \tag{5.2.38}$$

$$V_{x1} = \beta_1 V_{y1} \tag{5.2.39}$$

$$V_{x2} = \beta_2 V_{y2} . \tag{5.2.40}$$

The current equation of the passive components of the circuit shown in Fig. 5.2, can be written as

$$I_{R_1} = \frac{V_2 - V_{y1}}{R_1} \tag{5.2.41}$$

$$I_{R_2} = \frac{V_3 - V_{x1}}{R_2} \tag{5.2.42}$$

$$I_{R_3} = -\frac{V_{x2}}{R_3} \tag{5.2.43}$$

$$I_{C_1} = sC_1(V_1 - V_{y1}) \tag{5.2.44}$$

$$I_{C_2} = sC_2(V_{y2}) . \tag{5.2.45}$$

Furthermore, the input currents are related with each other by the following equations

$$I_{z2} = \alpha_2 I_{x2} = \alpha_2 I_{R_3} \tag{5.2.46}$$

$$I_{z1} = -\alpha_1 I_{x1} = -\alpha_1 I_{R_2} = -I_{C_2} . \tag{5.2.47}$$

After rearranging the terms in the above equations, we obtain

$$I_{R_1} = \frac{V_2 - V_O}{R_1} \tag{5.2.48}$$

$$I_{R_2} = \frac{V_3 - \beta_1 V_O}{R_2} \tag{5.2.49}$$

$$I_{R_3} = -\frac{\beta_2 V_{y2}}{R_3} \tag{5.2.50}$$

$$I_{C_1} = sC_1(V_1 - V_O). \tag{5.2.51}$$

By writing a KCL equation at the input node of the circuit shown in Fig. 5.2, we obtain

$$I_{C_1} + I_{R_1} = I_{y1} + I_{z2}. \tag{5.2.52}$$

Substituting Eq. (5.2.36), (5.2.46) and (5.2.48) in Eq. (5.2.51) gives

$$-\alpha_2 \frac{V_{x2}}{R_3} = sC_1(V_1 - V_O) + \frac{V_2 - V_O}{R_1} \tag{5.2.53}$$

$$V_{x2} = -\frac{1}{\alpha_2}\left[\ sC_1R_3(V_1 - V_O) + R_3\frac{V_2 - V_O}{R_1}\ \right]. \tag{5.2.54}$$

Assuming that $I_{z1} = -\alpha_1 I_{x1}$, then we obtain

$$V_{y2} = \alpha_1\left(\frac{V_3 - \beta_1 V_O}{sC_2R_2}\right). \tag{5.2.55}$$

Furthermore, assuming that $V_{x2} = \beta_2 V_{y2}$, then we obtain

$$\beta_2\alpha_1\left(\frac{V_3 - \beta_1 V_O}{sC_2R_2}\right) = -\frac{1}{\alpha_2}\left[\ sC_1R_3(V_1 - V_O) + R_3\frac{V_2 - V_O}{R_1}\ \right]. \tag{5.2.56}$$

After rearranging the terms in the above equation, the transfer function can be written as follows:

$$D(s) = s^2 R_1R_2R_3C_1C_2 + sR_2R_3C_2 + \alpha_1\alpha_2\beta_1\beta_2R_1. \tag{5.2.57}$$

Using Eq. (5.2.57), the natural frequency and the quality factor can be written as

$$\omega_o = \sqrt{\frac{\alpha_1 \alpha_2 \beta_1 \beta_2}{R_2 R_3 C_1 C_2}} \tag{5.2.58}$$

$$Q = \sqrt{\frac{\alpha_1 \alpha_2 \beta_1 \beta_2 C_1}{C_2 R_2 R_3}} R_1 . \tag{5.2.59}$$

It should be noted that, the subscripts of β and α in the above equations refer to the number of each current conveyor that is shown in Fig. 5.2. Also, the undamped natural frequency is independent from the active parameters, α and β.

5.3 SENSITIVITY ANALYSIS

The ideal sensitivities of the natural frequency and the quality factor with respect to passive components are calculated using Eqs. (5.2.31) and (5.2.32) as follows:

$$S_{R_1}^{\omega} = 0 \tag{5.3.1}$$

$$S_{R_2}^{\omega} = S_{R_3}^{\omega} = -\frac{1}{2} \tag{5.3.2}$$

$$S_{C_1}^{\omega} = S_{C_2}^{\omega} = -\frac{1}{2} \tag{5.3.3}$$

$$S_{R_1}^{Q} = 1 \tag{5.3.4}$$

$$S_{R_2}^{Q} = -\frac{1}{2} \tag{5.3.5}$$

$$S_{R_3}^{Q} = -\frac{1}{2} \tag{5.3.6}$$

$$S_{C_1}^{Q} = \frac{1}{2} \tag{5.3.7}$$

$$S_{C_2}^{Q} = \frac{1}{2} . \tag{5.3.8}$$

From the above calculations, it can be seen that the magnitude of all sensitivities are smaller than or equal to 1.

The non-ideal sensitivities of the natural frequency and the quality factor with respect to passive components are calculated using Eqs. (5.2.58) and (5.2.59) as follows:

$$S_{R_1}^{\omega}=0 \tag{5.3.9}$$

$$S_{R_2}^{\omega}=S_{R_3}^{\omega}=-\frac{1}{2} \tag{5.3.10}$$

$$S_{C_1}^{\omega}=S_{C_2}^{\omega}=-\frac{1}{2} \tag{5.3.11}$$

$$S_{\alpha_1}^{\omega}=S_{\alpha_2}^{\omega}=\frac{1}{2} \tag{5.3.12}$$

$$S_{\beta_1}^{\omega}=S_{\beta_2}^{\omega}=\frac{1}{2} \tag{5.3.13}$$

$$S_{R_1}^{Q}=1 \tag{5.3.14}$$

$$S_{R_2}^{Q}=-\frac{1}{2} \tag{5.3.15}$$

$$S_{R_3}^{Q}=-\frac{1}{2} \tag{5.3.16}$$

$$S_{C_1}^{Q}=\frac{1}{2} \tag{5.3.17}$$

$$S_{C_2}^{Q}=-\frac{1}{2} \tag{5.3.18}$$

$$S_{\alpha_1}^{Q}=S_{\alpha_2}^{Q}=\frac{1}{2} \tag{5.3.19}$$

$$S_{\beta_1}^{Q}=S_{\beta_2}^{Q}=\frac{1}{2}. \tag{5.3.20}$$

Again, if passive component values are chosen appropriately, then the magnitude of the sensitivities due to non-ideal effects will also be small than or equal to 1.

5.4 EXPERIMENTAL AND SIMULATION RESULTS

The validity of the filter proposed by Sagbas et al. (Sagbas et al., 2005) shown in Fig. 5.2 has been verified both experimentally and through PSPICE simulations. For experimental verification, the AD844 IC manufactured by Analog Devices was used (Analog Devices, 1990). Since AD844 can realize only positive-type second generation current conveyors (CCII+s) the CCII- had to be constructed from two positive-type second generation current conveyors (Svoboda et al., 1991). The circuit was supplied with symmetrical voltages of $V_{cc} = 12\text{ V}$ and $V_{ee} = -12\text{ V}$, respectively and was designed using the parameters shown in Table 5.1.

Table 5.1 Design parameters used for verifying the validity of the voltage mode MISO output filter using two current conveyors.

3dB cutoff frequency (f_O) (kHz)	C_2 (nF)	C_4 (nF)	R_1 (kΩ)	R_2 (kΩ)	R_3 (kΩ)
112.5.	**1**	**1**	**1**	**2**	**1**

The simulations were carried out using the model parameters of AD844 from the built in library of PSPICE simulation program.

The simulation and experimental results for the second-order low-pass, high-pass, and band-pass filters are shown in Fig. 5.8 through Fig. 5.10, respectively. Furthermore, Fig. 5.11 shows the filter responses for different configurations on a single graph for comparison. Although, the experimental and simulation results well fit into one another over a wide range of frequency, some discrepancies can be observed in the results. These discrepancies are related with the non-ideal characteristics of AD844 IC and the experimental equipment.

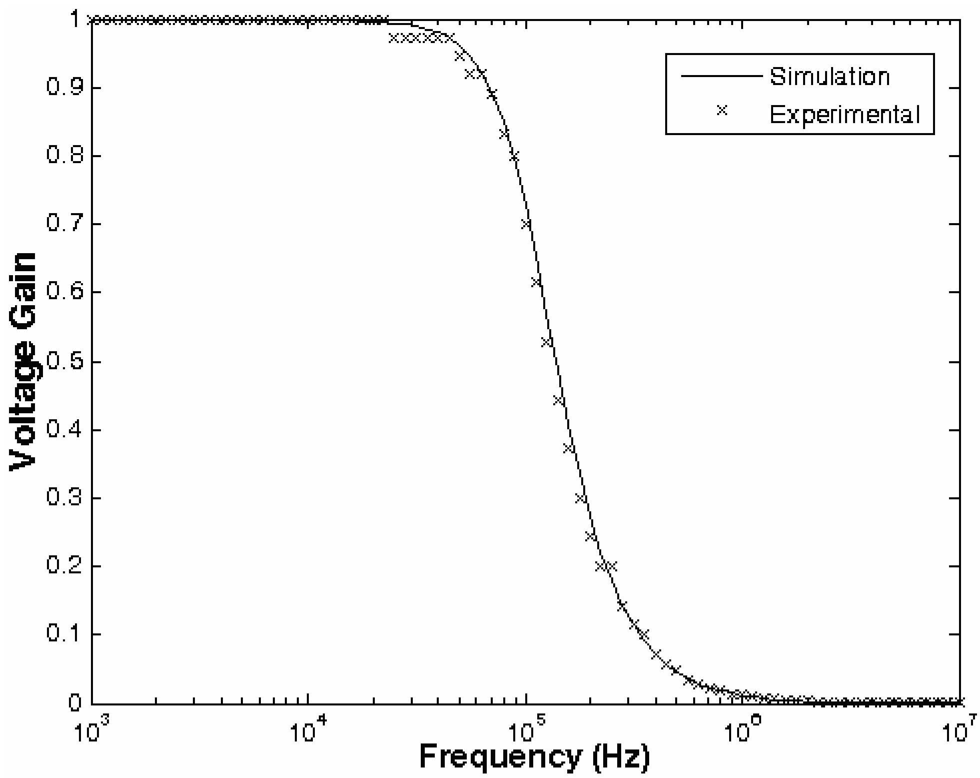

Figure 5.8 Simulation and experimental results for the low-pass (LP) filter proposed by Sagbas et al. (Sagbas et al., 2005).

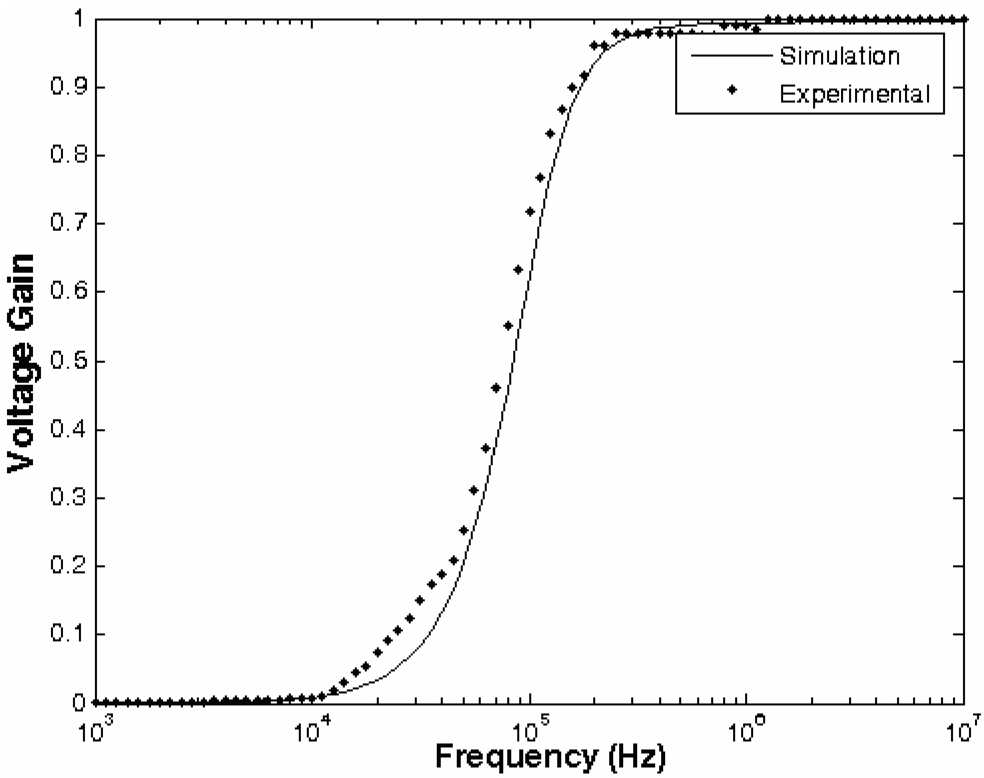

Figure 5.9 Simulation and experimental results for the high-pass (HP) filter proposed by Sagbas et al. (Sagbas et al., 2005).

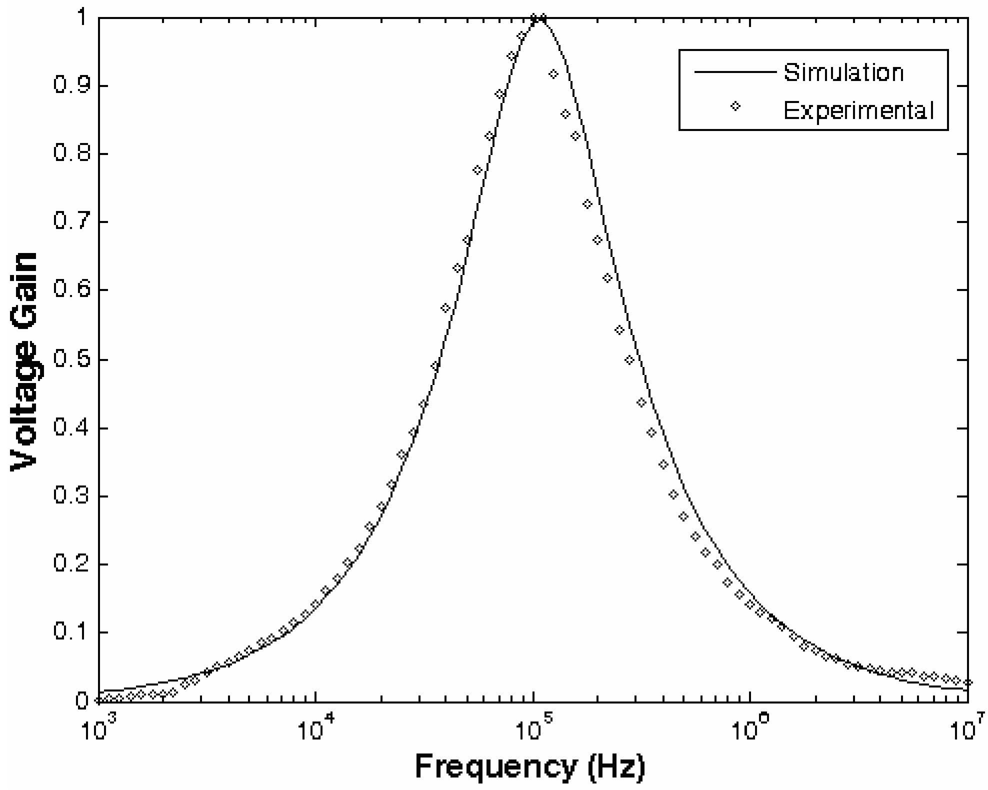

Figure 5.10 Simulation and experimental results for the band-pass (BP) filter proposed by Sagbas et al. (Sagbas et al., 2005).

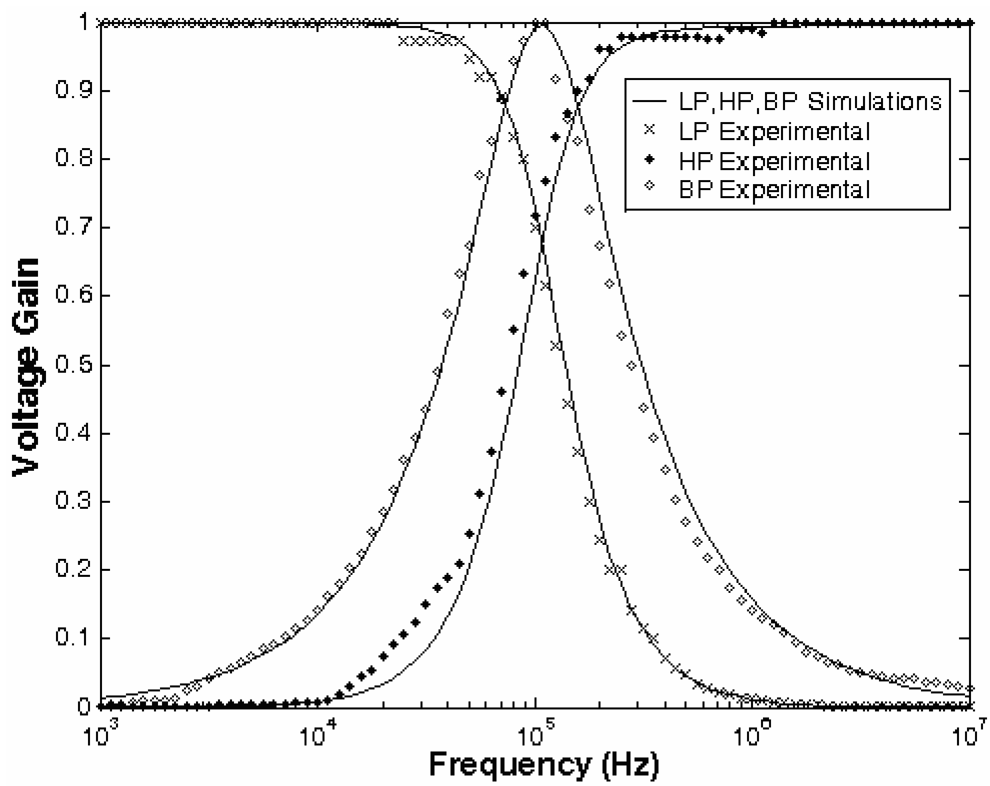

Figure 5.11 Comparison of simulation and experimental results for the LP, HP, and BP filters proposed by Sagbas et al. (Sagbas et al., 2005).

CHAPTER 6

A NEW CURRENT MODE MULTIFUNCTION FILTER USING TWO DUAL-OUTPUT CURRENT CONTROLLED CONVEYORS

6.1 INTRODUCTION

In this Chapter, a new current-mode multifunction filter that realizes three basic filter functions at its high impedance outputs with minimum number of passive elements is proposed. The proposed filter consists of only two passive elements (two capacitors) and two dual-output second generation current controlled conveyors (DO-CCCIIs). It has a single-input and three high impedance outputs. Each output provides a different filter response, namely low-pass (LP), high-pass (HP), and band-pass (BP). The sensitivity analysis is performed for ideal and non-ideal filter configurations. The validity of the proposed filter is verified through PSPICE simulations.

The new circuit offers the following attractive features:

(i) Three different filter responses (LP, HP, and BP) at each output.

(ii) All capacitors are grounded which makes the filter more suitable for IC integration.

(iii) High impedance at the output except the HP case, which enables the filter for easy cascadability without the need of any supplementary buffer circuits.

(iv) Very low active and passive filter sensitivities.

(v) Use of minimum number of elements (two capacitors, two DO-CCCIIs).

Section 6.2 presents the proposed multifunction filter function for both ideal and non-ideal cases. In Section 6.3, the sensitivity analysis of the proposed filters is presented. In Section 6.4, PSPICE simulation results are presented.

6.2 CIRCUIT DESCRIPTION AND ANALYSIS OF THE PROPOSED FILTER

6.2.1 Ideal Case

The block diagram of a dual-output second generation current controlled conveyor (DO-CCCII) is shown in Fig. 6.1. The terminal equations for the ideal case can be written as (Soliman, 1997), (Fabre et al., 1995).

$$V_x = V_y + I_x R_x \tag{6.2.1}$$

$$I_y = 0 \tag{6.2.2}$$

$$I_{z+} = I_x \tag{6.2.3}$$

$$I_{z-} = -I_x \tag{6.2.4}$$

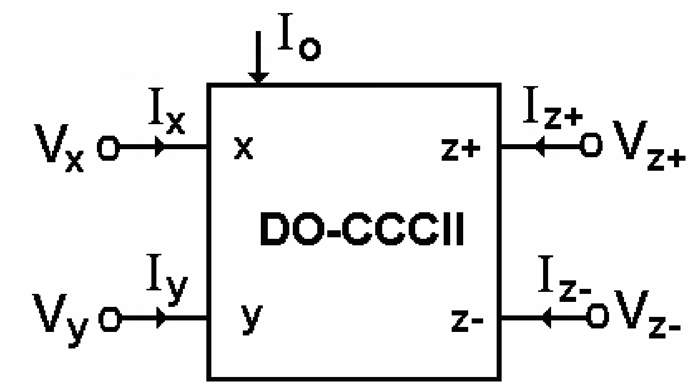

Figure 6.1 Block diagram of a dual-output second generation current controlled conveyor (DO-CCCII).

The input impedances of the ideal DO-CCCII are infinite at terminal y and R_x at terminal *x*, respectively. The terminal *z* that is equivalent to a current generator possesses infinite output impedance. Electronic adjustability of the DO-CCCII is attributed to the dependence of the parasitic resistance on the bias current of the current conveyor at terminal *x*. The parasitic *x*-input resistance, R_x for $I_x(t) << 2I_O$ can be obtained as follows: $R_x = \frac{kT/q}{2I_O} = \frac{V_T}{2I_O}$ where, *k* is the Boltzmann's constant, *T* is the temperature, *q* is the magnitude of the electronic charge and V_T is the thermal voltage.

Hence, R_x can be controlled by varying the bias current I_O. In addition to this, the quality factor, Q and natural frequency, ω_O depend on R_x which makes these parameters adjustable electronically.

The proposed current mode DO-CCCII multifunction filter is shown in Fig.6.2. This circuit is analyzed using the terminal equations given by Eqs. (6.2.1) through (6.2.4) as follows:

$$I_{x1} = I_{z1+} = -I_{z1-} = I_{BP} \tag{6.2.5}$$

$$I_{x2} = I_{z2+} = -I_{z2-} = I_{LP} \tag{6.2.6}$$

$$V_{y1} = V_{x2} = 0 \tag{6.2.7}$$

$$V_{x1} = V_{y1} + I_{x1}R_{x1} = I_{BP}R_{x1} \tag{6.2.8}$$

$$V_{y2} = I_{x2}R_{x2} = -I_{LP}R_{x2} \tag{6.2.9}$$

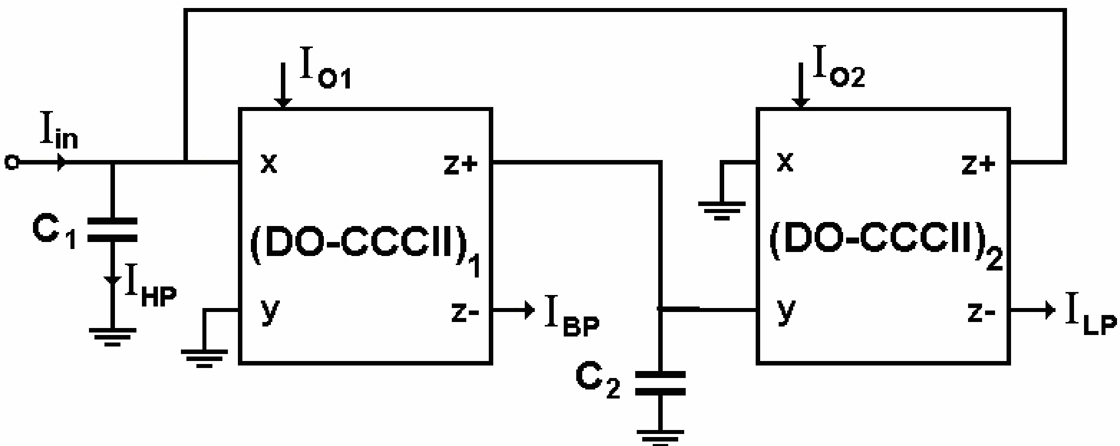

Figure 6.2 Circuit diagram of the proposed current-mode DO-CCCII multifunction filter.

By writing a KCL equation at the input node of the proposed circuit shown in Fig. 6.2, we obtain

$$I_{in} = I_{HP} + I_{BP} + I_{LP} \tag{6.2.10}$$

By writing node voltage equations for the proposed circuit shown in Fig. 6.2, we obtain

$$V_{x1} = \frac{I_{HP}}{sC_1} \tag{6.2.11}$$

$$V_{y2} = -\frac{I_{BP}}{sC_2} \tag{6.2.12}$$

When Eq. (6.2.8) and Eq. (6.2.11) are equated, we obtain

$$I_{BP}R_{x1} = \frac{I_{HP}}{sC_1} \tag{6.2.13}$$

Equation (6.2.13) can be simplified as follows:

$$I_{BP} = \frac{I_{HP}}{sC_1R_{x1}} \tag{6.2.14}$$

Equating Eq. (6.2.9) to Eq. (6.2.12) yields

$$I_{LP}R_{x2} = \frac{I_{BP}}{sC_2} \tag{6.2.15}$$

Equation (6.2.15) can be simplified as follows:

$$I_{BP} = sC_2R_{x2}I_{LP} \tag{6.2.16}$$

After substituting Eq. (6.2.14) and Eq. (6.2.16) into Eq. (6.2.10), the transfer function of the circuit at different outputs is found as follows:

$$\frac{I_{LP}}{I_{in}} = \frac{1}{s^2 R_{x1} R_{x2} C_1 C_2 + s R_{x2} C_2 + 1} \quad (6.2.17)$$

$$\frac{I_{HP}}{I_{in}} = \frac{s^2 R_{x1} R_{x2} C_1 C_2}{s^2 R_{x1} R_{x2} C_1 C_2 + s R_{x2} C_2 + 1} \quad (6.2.18)$$

$$\frac{I_{BP}}{I_{in}} = \frac{s R_{x2} C_2}{s^2 R_{x1} R_{x2} C_1 C_2 + s R_{x2} C_2 + 1} \quad (6.2.19)$$

Equations (6.2.17), (6.2.18), and (6.2.19) show that the proposed filter produces LP, HP, and BP responses simultaneously at its high impedance outputs. The natural frequency and the quality factor of the proposed circuit are calculated from the denominator of the transfer functions as follows:

$$\omega_o = \frac{1}{\sqrt{R_{x1} R_{x2} C_1 C_2}} \quad (6.2.20)$$

$$Q = \sqrt{\frac{R_{x1} C_1}{R_{x2} C_2}} \quad (6.2.21)$$

6.2.2 Non-ideal Case

Taking the non-idealities into account, the terminal equations of the DO-CCCII-shown in Fig. 6.1 can be written as

$$V_x = \beta V_y + I_x R_x \quad (6.2.22)$$

$$I_y = 0 \quad (6.2.23)$$

$$I_{z+} = \alpha I_x \quad (6.2.24)$$

$$I_{z-} = -\alpha I_x \quad (6.2.25)$$

where, $\beta = 1 - \varepsilon_V$ and $\alpha = 1 - \varepsilon_i$. ε_V ($|\varepsilon_V| << 1$) and ε_i ($|\varepsilon_i| << 1$) denote the voltage and current tracking errors, respectively (Smith et al, 1970).

Using Eq. (6.2.22) through (6.2.25), the terminal equations for the circuit shown in Fig. 6.2 become

$$\alpha_1 I_{x1} = I_{z1+} = -I_{z1-} = I_{BP} \tag{6.2.26}$$

$$\alpha_2 I_{x2} = I_{z2+} = -I_{z2-} = I_{LP} \tag{6.2.27}$$

$$V_{y1} = V_{x2} = 0 \tag{6.2.28}$$

$$V_{x1} = \beta_1 V_{y1} + I_{x1} R_{x1} = I_{x1} R_{x1} = I_{BP} R_{x1} / \alpha_1 \tag{6.2.29}$$

$$V_{y2} = I_{x2} R_{x2} / \beta_2 = -I_{LP} R_{x2} / \alpha_2 \beta_2 \tag{6.2.30}$$

By writing a KCL equation at the input node of the circuit shown in Fig. 6.2, we obtain

$$I_{in} = I_{HP} + \frac{I_{BP}}{\alpha_1} + I_{LP} \tag{6.2.31}$$

By writing node voltage equations for the circuit shown in Fig. 6.2, we obtain

$$V_{x1} = \frac{I_{HP}}{sC_1} \tag{6.2.32}$$

$$V_{y2} = -\frac{I_{BP}}{sC_2} \tag{6.2.33}$$

Equating Eq. (6.2.29) to Eq. (6.2.32), we obtain

$$\frac{I_{BP} R_{x1}}{\alpha_1} = \frac{I_{HP}}{sC_1} \tag{6.2.34}$$

Equation (6.2.13) can be simplified as follows:

$$I_{BP} = \frac{\alpha_1}{sC_1 R_{x1}} I_{HP} \tag{6.2.35}$$

Equating Eq. (6.2.33) to Eq. (6.2.30) yields

$$\frac{I_{LP} R_{x2}}{\alpha_2 \beta_2} = \frac{I_{BP}}{sC_2} \tag{6.2.36}$$

Equation (6.2.36) can be simplified as follows:

$$I_{BP} = \frac{sC_2 R_{x2} I_{LP}}{\alpha_2 \beta_2} \tag{6.2.37}$$

After substituting Eq. (6.2.35) and Eq. (6.2.37) into Eq. (6.2.31), the transfer function of the circuit at different outputs is found as follows:

$$\frac{I_{LP}}{I_{in}} = \frac{\alpha_1 \alpha_2 \beta_2}{s^2 R_{x1} R_{x2} C_1 C_2 + s\alpha_1 R_{x2} C_2 + \alpha_1 \alpha_2 \beta_2} \tag{6.2.38}$$

$$\frac{I_{HP}}{I_{in}} = \frac{s^2 R_{x1} R_{x2} C_1 C_2}{s^2 R_{x1} R_{x2} C_1 C_2 + s\alpha_1 R_{x2} C_2 + \alpha_1 \alpha_2 \beta_2} \tag{6.2.39}$$

$$\frac{I_{BP}}{I_{in}} = \frac{s\alpha_1 R_{x2} C_2}{s^2 R_{x1} R_{x2} C_1 C_2 + s\alpha_1 R_{x2} C_2 + \alpha_1 \alpha_2 \beta_2} \tag{6.2.40}$$

Equations (6.2.17), (6.2.18), and (6.2.19) show that the proposed filter produces LP, HP, and BP responses simultaneously at its high impedance outputs. The natural frequency and the quality factor of the proposed circuit are calculated from the denominator of the transfer functions as follows:

$$\omega_o = \sqrt{\frac{\alpha_1 \alpha_2 \beta_2}{R_{x1} R_{x2} C_1 C_2}} \tag{6.2.41}$$

$$Q = \sqrt{\frac{\alpha_2 \beta_2 R_{x1} C_1}{\alpha_1 R_{x2} C_2}} \tag{6.2.42}$$

6.3 SENSITIVITY ANALYSIS

The ideal sensitivities of the natural frequency and the quality factor with respect to passive components are calculated using Eqs. (6.2.20) and (6.2.21) as follows

$$S_{R_{x1}}^{\omega_o} = S_{R_{x2}}^{\omega_o} = S_{C_1}^{\omega_o} = S_{C_2}^{\omega_o} = -\frac{1}{2} \tag{3.3.1}$$

$$S_{R_{x1}}^{Q} = S_{C_1}^{Q} = \frac{1}{2} \tag{3.3.2}$$

$$S_{R_{x2}}^{Q} = S_{C_2}^{Q} = -\frac{1}{2} \tag{3.3.3}$$

From the above calculations, it can be seen that the magnitude of all sensitivities are constant and equal to 1/2.

Using Eqs. (6.2.41) and (6.2.42), the non-ideal sensitivities can be calculated as follows:

$$S_{R_{x1}}^{\omega_o} = S_{R_{x2}}^{\omega_o} = S_{C_1}^{\omega_o} = S_{C_2}^{\omega_o} = -\frac{1}{2} \tag{3.3.4}$$

$$S_{\alpha_1}^{\omega_o} = S_{\alpha_2}^{\omega_o} = S_{\beta_2}^{\omega_o} = \frac{1}{2} \tag{3.3.5}$$

$$S_{\alpha_2}^{Q} = S_{\beta_2}^{Q} S_{R_{x1}}^{Q} = S_{C_1}^{Q} = \frac{1}{2} \tag{3.3.6}$$

$$S_{\alpha_1}^{Q} = S_{R_{x2}}^{Q} = S_{C_2}^{Q} = -\frac{1}{2} \tag{3.3.7}$$

Again, from the above calculations, it can be seen that all sensitivities due to non-ideal effects are constant and equal to 1/2.

6.4 SIMULATION AND RESULTS

The validity of the proposed filter shown in Fig. 6.2 has been verified through PSPICE simulations. Each DO-CCCII was realized using BJT implementation shown in Fig. 2.6 (Fabre et al., 1996). For this simulation, the passive components were chosen as, $C_1 = 1\ \text{nF}$ and $C_2 = 1\ \text{nF}$. The circuit was supplied with symmetrical voltages of $\text{V}_{\text{cc}} = 2.5\ \text{V}$ and $\text{V}_{\text{ee}} = -2.5\ \text{V}$. The center frequency of the filter was set to 112.5 kHz by changing bias currents I_{O1} to $13\ \mu\text{A}$ and I_{O2} to $6.5\ \mu\text{A}$, respectively.

The simulations were carried out using the model parameters of NPN and PNP transistors given in Table 6.1.

Table 6.1 Model parameters for NPN and PNP transistors used in PSPICE simulations.

Parameter	PNP	NPN
IS	100.000000E-18 A	100.000000E-18 A
BF	100	100
NF	1	1
BR	1	1
NR	1	1
CN	2.2	2.42
D	0.52	0.87

The parameters shown in Table 6.1 are described as follows:

- IS: Transport saturation current,
- BF: Ideal maximum forward beta,
- NF: Forward current emission coefficient,
- BR: Ideal maximum reverse beta,
- NR: Reverse current emission coefficient,
- CN: Quasi-saturation temperature coefficient for hole mobility,
- D: Quasi-saturation temperature coefficient for scattering-limited hole carrier velocity

PSPICE simulation results for the proposed multifunction filter are shown in Fig. 6.3, through Fig. 6.5, respectively. Fig. 6.6 shows all simulation results on a single graph for comparison. From these figures, it can be observed that the three basic filter functions, namely; LP, HP, and BP filter can be realized accurately using the proposed configuration.

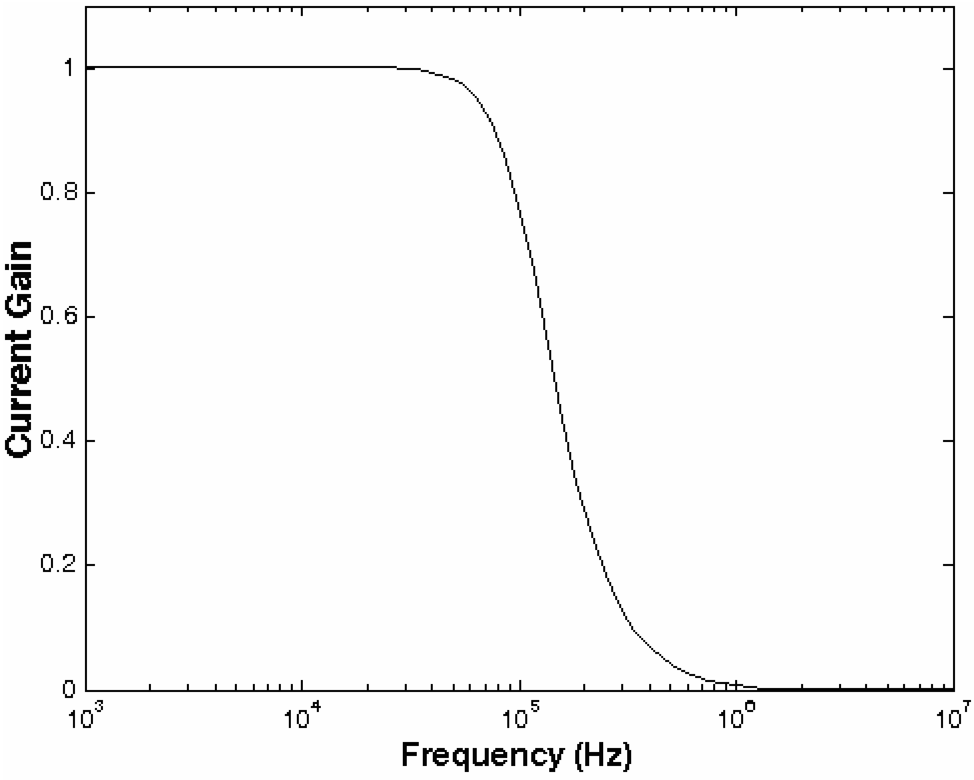

Figure 6.3 Simulation result for the proposed low-pass (LP) filter.

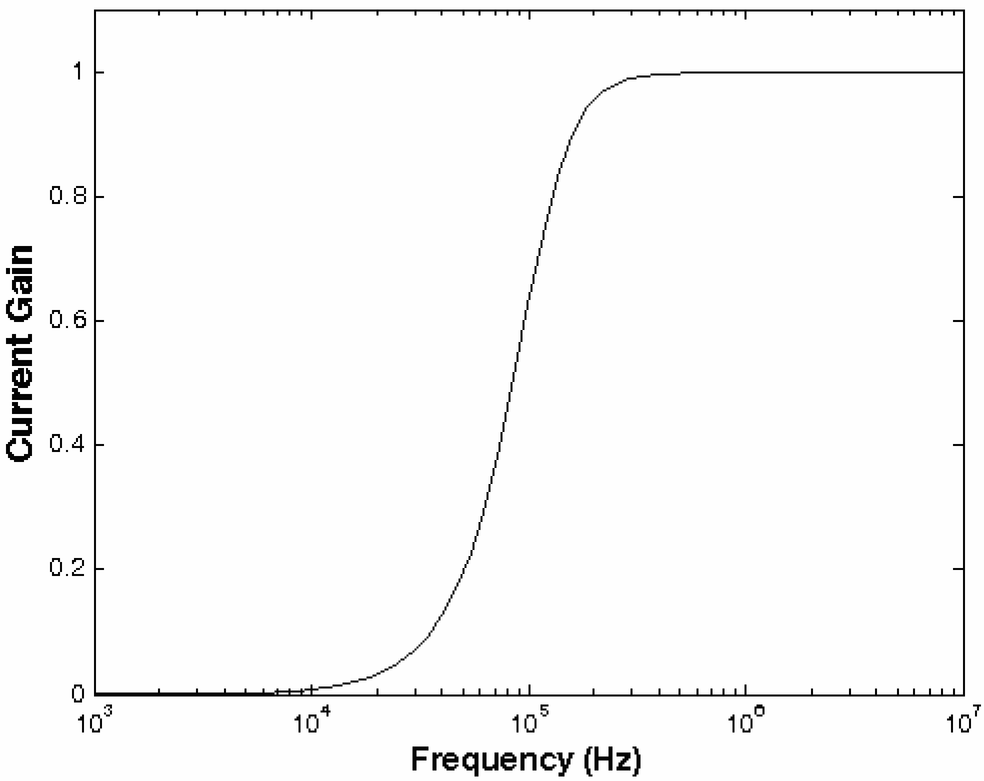

Figure 6.4 Simulation result for the proposed high-pass (HP) filter.

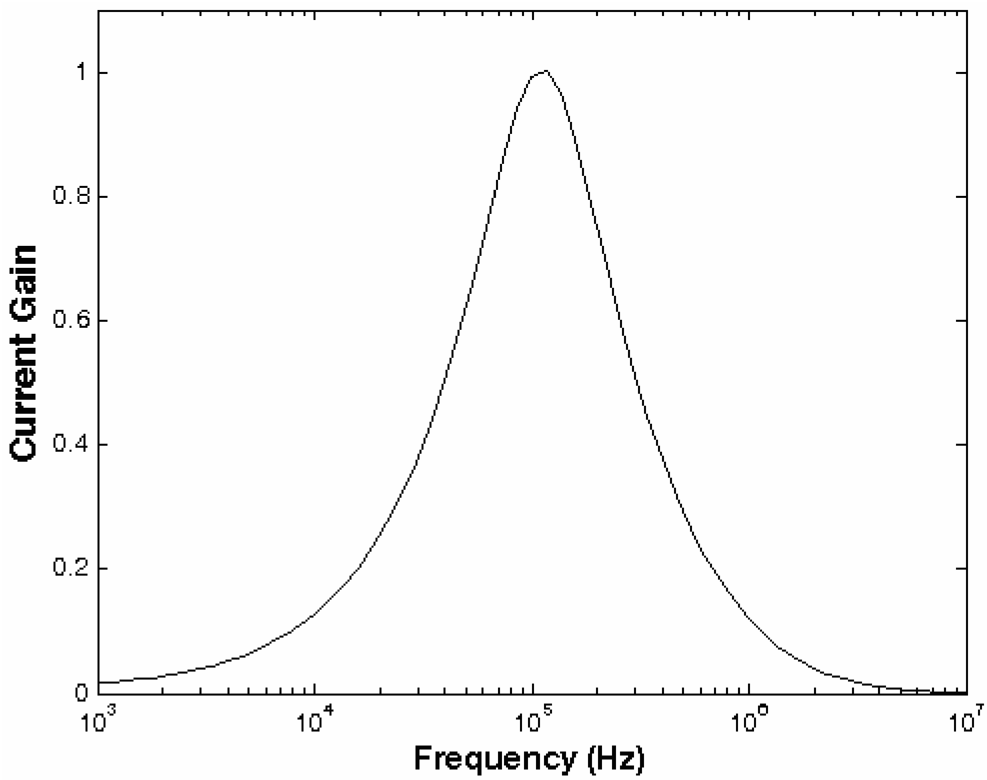

Figure 6.5 Simulation result for the proposed band-pass (BP) filter.

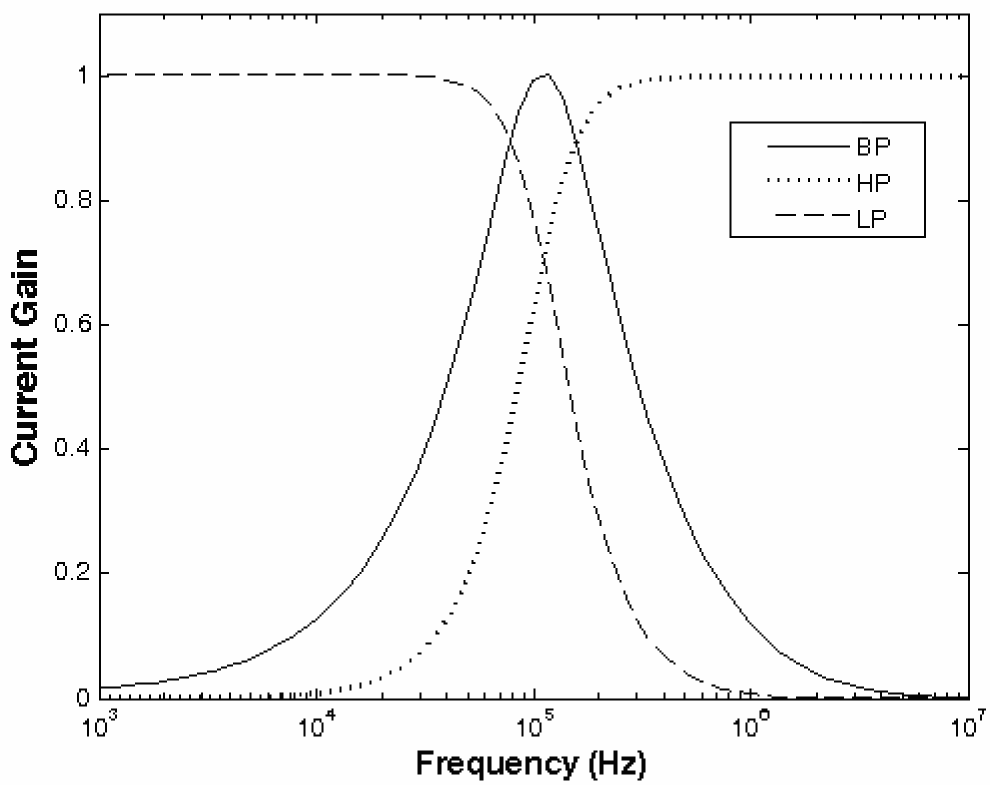

Figure 6.6 Comparison of simulation result for the proposed LP, HP, and BP filters.

CHAPTER 7

CONCLUSIONS

In this thesis, we have focused on the experimental verification of voltage mode second order multiple input single output (MISO) filters and design of both voltage-mode and current-mode second-order filters using current conveyors. We have presented three voltage-mode MISO second-order filters using CCIIs and one current-mode multifunctional second-order filter using DO-CCCII.

In Chapter three, a new voltage-mode multiple-input single-output multifunction (MISO) filter using a single negative type second generation current conveyor (CCII-) was proposed. The proposed multifunction filter was verified both experimentally and through simulations. For experimental verification, the commercially available current feedback operational amplifier AD844 manufactured by Analog Devices was used. The simulations were carried out using the model parameters of AD844 from the built-in library of PSPICE simulation program. The experimental and simulation results for low-pass, band-pass, high-pass, and band-reject have a very good correlation with each other. Small discrepancies are related with the non-ideal characteristics of AD844 IC and the experimental equipment. The proposed filter has the following advantages: (i) Voltage-mode circuits using conventional operational amplifier have the disadvantage of severely reduced bandwidth at higher gains because of the op-amp's fixed gain-bandwidth product. These disadvantages can be eliminated by using current conveyors and current conveyor based active elements (Wilson et al., 1990), (Wandsworth et al., 1989); (ii) Realization of all the basic filter functions: low-pass, high-pass, band-pass, band-reject, and all-pass; (iii) Low passive and active sensitivities; (iv) High output impedance; (v) Ability to adjust the natural frequency and quality factor; (vi) High quality factor.

In Chapter four, the experimental verification of a voltage-mode multiple-input single-output multifunction filter using a single current conveyor proposed by Sagbas (Sagbas, 2003) was presented. The current conveyor was realized by a commercially available current feedback operational amplifier AD844 of Analog Devices. The experimental results were compared with PSPICE simulations. The experimental and simulation results for low-pass, band-pass, high-pass, and band-reject have a very good correlation with each other. Small discrepancies are related with the non-ideal characteristics of AD844 IC and the experimental equipment. Effect of the non-idealities and the sensitivity analysis of the proposed filter were also examined. The multifunction filter has the following advantages: (i) The use of current conveyor eliminates the disadvantage possessed by voltage-mode circuits using operational amplifiers (Wilson et al., 1990), (Wandsworth et al., 1989); (ii) Realization of all the basic filter functions such as low-pass, high-pass, band-pass, band-reject, and all-pass; (iii) Low passive and active sensitivities; (iv) High output impedance; (v) Undamped natural frequency is independent from the active parameters; (vi) Use of positive-type second generation current conveyor which is more suitable than negative-type second generation current conveyor in IC technology; (vii) Ability to adjust the natural frequency and quality factor.

In Chapter five, the experimental verification of a voltage-mode multiple-input single-output multifunction filter using two current conveyors proposed by Sagbas et al. (Sagbas et al., 2005) was presented. The current conveyors were realized by commercially available current feedback operational amplifier AD844 of Analog Devices. The experimental results were compared with PSPICE simulations. The experimental and simulation results for low-pass, band-pass, high-pass, and band-reject have a very good correlation with each other. Again the small discrepancies are related with the non-ideal characteristics of AD844 IC and the experimental equipment. Effect of the non-idealities and the sensitivity analysis of the proposed filter were also examined. The multifunction filter has the following advantages: (i) Voltage-mode circuits using conventional operational amplifier have the disadvantage of severely reduced bandwidth at higher gains, because of the op-amp’s fixed gain-bandwidth product. These disadvantages can be eliminated by using current conveyors and current conveyor based active elements; (ii) Realization of all the basic filter functions: low-pass, high-pass, band-pass and band-reject; (iii) Low passive and active sensitivities;

(iv) High output impedance; (v) Ability to adjust the natural frequency and quality factor.

In Chapter six, a new current-mode multifunction filter that realizes three basic filter functions at its high impedance outputs with minimum number of passive elements was proposed. The sensitivity analysis was performed for ideal and non-ideal filter configurations. The validity of the proposed filter was verified through PSPICE simulations. The new circuit offers the following attractive features: (i) Three different filter responses (LP, HP, and BP) at each output; (ii) All capacitors are grounded which makes the filter more suitable for IC integration; (iii) High impedance at the output, which enables the filter for easy cascadability without the need of any supplementary buffer circuits. High output impedance; (iv) Undamped natural frequency is independent from the active parameters; (v) Use of minimum number of elements (two capacitors, two DO-CCCIIs).

REFERENCES

Abuelma'tti, M. T. and Khan, M. H., "Low component current-mode universal filter", *Electronics Letters*, Vol. 31, pp. 2160-2161, 1995.

Abuelma'atti, M. T. and Shabra, M. H., "A novel current conveyor based universal current-mode filter", *Microelectronics Journal*, Vol.27, pp. 471-475, 1996.

Abuelma'tti, M. T., Khan, M. H., and Al-Zaher, H.A., "Simulation of active-only floating inductance", *Frequenz,* Vol.52, pp. 161-164, 1998.

Analog Devices: '*Linear products data book*', Norwood, MA, 1990.

Becvar D. "Novel universal active block: a universal current conveyor ", *Proc. of ISCAS 2000*, Geneva, pp. 471-474, 2000.

Chang, C. M. and Chen, P. C., "Universal active current filter with three inputs and one output using current conveyors", *International Journal of Electronics*, Vol.71, pp. 817-819, 1991.

Chang, C. M. and Chen, P. C., "Realization of current-mode transfer function using second-generation current conveyors", *International Journal of Electronics*, Vol.71, pp. 809-815, 1991.

Chang, C. M. and Chen, P. C., "Universal capacitor-grounded voltage-mode filter with three inputs and a single output", *International Journal of Electronics*, Vol.90, pp. 401-406, 2003.

Chang, C. M., "Novel universal current-mode filter with single input and three outputs using only five current conveyors", *Electronics* Letters, Vol. 29, pp. 2005-2007, 1993.

Chang, C. M., "Current mode low-pass, band-pass and high-pass biquads using two CCIIs", *Electronics Letters*, Vol. 29, pp. 2020-2021, 1993.

Chang, C. M., "Universal active current filter with single input and three outputs using CCIIs", *Electronics Letters*, Vol. 29, pp. 1932-1933, 1993.

Chang, C. M., Chen C. C. and Wang, H. Y., "Universal active current filter with three inputs using current conveyors-part 2", *International Journal of Electronics*, Vol. 76, pp. 87-89, 1994.

Chang, C. M., Lee, M. S: ‘Comment: Universal voltage-mode filter with three inputs and one output using three current conveyors and one voltage follower’, *Electronics Letters*, Vol. 31, pp. 353, 1996.

Chang C.M., “Universal active current filter with three inputs and one output using plus type CCIIs”, *Electronics Letters*, Vol. 33, No 14, pp. 1207-1208, 1997.

Chang, C. M. and TU, S. H., ”Universal voltage-mode filter with four inputs and one output using two CCII+s”, *International Journal of Electronics*, Vol. 86, No. 3, pp. 305-309, 1999.

Chen, P. C., “Universal active current filter with three inputs and one output using current conveyor”, *International Journal of Electronics*, Vol. 71, pp. 817-819, 1991.

Chiu, W. “CMOS Differential difference current conveyors and their applications”, *IEE Proc. Circuits Devices Syst*., Vol. 143, No.2, pp. 91-96, 1996.

Chong, C. P. and K. C. Smith, “Biqadratic filter sections employing a single current conveyor”, *Electronics Letters,* Vol. 22, No. 22, pp. 1162-1164, 1986.

Elwan, O. E., and Soliman, A. M., “A novel CMOS current conveyor realization with an electronically tunable current-mode filter suitable for VLSI”, *IEEE Trans-II*, Vol. CAS-43, pp. 663-670, 1996.

Fabre A., “Third generation current conveyor: a new helpful active element”, *Electronics Letters*, Vol.31, pp. 338-339, 1995.

Fabre, A., Saaid, O., Wiest, F. and Boucheron, C., “Current controlled bandpass filter based on translinear conveyors”, *Electronics Letters*, Vol.31 , pp. 1727-1728, 1995.

Fabre, A., Saaid, O., Wiest, F. and Boucheron, C., “High frequency application based on a new current controlled conveyor”, *IEEE Transactions on Circuits and Systems-I: Fundamental Theory and Applications,* Vol. 43, pp. 82-91, 1996.

Gunes, E. O. and Anday, F., “Realizaion of current-mode universal filter using CFCCIIps”, *Electronics Letters*, Vol. 31, No. 12, pp. 1081-1082, 1996.

Higashimura, M., “Realization of voltage-mode biquads using CCII+”, *Electronics Letters*, Vol. 27, pp. 1354-1346, 1991.

Horng, J. W. Weng R.-O. Lee M.-H. and Chang C.W., “Universal active current filter using two multiple current output OTAs and one CCIII”, *International Journal of Electronics*, Vol. 82, 1996.

Horng, J. W., Lee M. H., Cheng, H. C., Chang, C. W., “New CCII based voltage mode universal biquadratic filter”, *International Journal of Electronics*, Vol. 82, pp. 151-155, 1997.

Horng, J. W., CHANG, C.K., and CHU, J.M., “Voltage-mode universal biquadratic filter using single current feedback amplifier”, *IEICE Tran. On Fundamental of Electronics Commun. And Com. Science*, Vol. E85A, pp. 1970-1973, 2002.

Horng, J. W., CHIU W.Y., and WEI H.Y., “Voltage-mode highpass, bandpass and lowpass filters using DDCCs”, *International Journal of Electronics*, Vol. 91, pp. 461-464, 2004.

Horng, J. W., HOU C.L., CHANG C. M., CHUNG W.Y., and WEI H.Y., “Voltage-mode h universal biquadratic filters with one input and five outputs using MOCCIIs”, *Computers and Electrical Engineering*, Vol. 31, pp. 190-202, 2005.

Horng, J. W., “New Configuration for Realizing Universal Voltage-Mode Filter Using Two Current Feedback Amplifiers”, IEEE Trans*IEEE Trans. On Instrumentatşon and Measurement,* Vol. 49, No.5, 2000.

Horng, J. W., “High-input impedance voltage mode universal biquadratic filter using three plus type CCIIs”, *IEEE Trans. on Circuits and Systems*, Vol 48, No. 10, 2001.

Horng, J. W., “High-input impedance voltage-mode universal biquadratic filter using two OTAs and one CCII”, *International Journal of Electronics,* Vol. 49, pp. 185-191, 2003.

Horng, J. W., “High-input impedance voltage-mode universal biquadratic filters with three inputs using plus-type CCIIs”, *International Journal of Electronics,* Vol. 91, pp. 465-475, 2004.

Hou, C.L., Chen, R.D., Wu, Y.P. and Hu, P.CP., “Realization of grounded and floating immitance function simulators using current conveyors”, *International Journal of Electronics,* Vol. 74, pp. 917,923, 1993.

Hou, C. L. and Wu, J. S., “Universal cascadable current-mode biquad using only four CCIIs”, *International Journal of Electronics*, Vol. 82, pp. 125-129, 1997.

Hou, C.L., Huang, C.C., Lan, Y.S., Shaw,J.J., and Chang, C.M.., “Current-mode and voltage-mode universal biquads using a single current-feedback amplifier”, *International Journal of Electronics,* Vol. 86, pp. 929-932, 1999.

Ikeda, K., Tomita, Y., “Realization of current-mode biquadratic filter using CCIIs with current followers”, *Electronics and Communication in Japan*, Part 2, Vol. 77, No. 1, pp. 99-107, 1994.

Khan, I.A. and Ahmet, M.T., “Wide range electronically tunable multifunctional OTA-C filter for instrumentation applications”, *IEEE Trans. Instrum. Meas*, Vol. 36, pp. 13-17, 1987.

Khan, I. and Maheshewari, S., “Simple first order all-pass section using a single CCII”, *International Journal of Electronics*, Vol. 87, pp. 303-306, 2000.

Kumar, U., Shukla, S.K., "Recent developments in current conveyors and their applications", *IEE Proc. G.*, Vol. 16, pp. 47-52, 1985.

Kuntman, H., Çiçekoğlu, O., Özoğuz, S., and Karaçivi, B. "Universal Current-mode Filter Implemented with the modified third generation current conveyor", *Norsıg2000*, pp. 165-168, 2000.

Kwan, T. and Martin, K., "An adaptive analog continuous-time CMOS biquadratic filter", *IEEE J. Solid-State circuits*, Vol. 26, pp. 859-867, 1991.

Liu, S. I., Tsao, H.W. and Wu, J., "Cascadable current-mode single CCII biquad", *Electronics Letters*, Vol. 26, pp. 2005-2006, 1990.

Liu, S. I. and Yang Y.Y., "Higher-order immittance function synthesis using CCIIIs", *Electronics Letters*, Vol. 32, pp. 2295-2296, 1996.

Liu, S. I. and Lee, J. L.: "Voltage-mode universal filters using two current conveyors", *International Journal of Electronics*, Vol. 82, pp. 145-149, 1997.

Minaei, S., and Turkoz, S., "A new current-mode current controlled universal filter implemented from single-output current controlled conveyors", *Frequenz*, Vol. 54, pp. 138-140, 2000.

Minaei, S., and Turkoz, S., "A new current-mode current controlled universal filter with single input and three output currents", *International Journal of Electronics*, Vol. 88, pp. 915-922, 2001.

Minaei, S., Cicekoglu, O., Kutman, H., and Turkoz, S., "High output impedance current-mode lowpass, bandpass and highpass filters using current controlled conveyors", *International Journal of Electronics*, Vol. 8, pp. 915-922, 2001.

Minaei, S., Topcu, G., and Cicekoglu,O., "Low input impedance type multifunction filter using only active elements", *International Journal of Electronics*, Vol. 90, pp. 385-392, 2005.

Ozcan, S., Kuntman, H., and Cicekoglu, O., 'Multi-input single-output filter with reduced number of passive elements using single Current Conveyor', Computers and Electrical Engineering, Vol.29, No. 1, pp. 45-53, 2003.

Ozoguz, S. and Gunes, E. O., "Universal filter with three inputs using CCII", *Electronics Letters*, Vol. 32, pp. 2134-2135, 1996.

Ozuguz, S. and Acar, C., "Universal current mode filter with reduced number of active and passive components", *Electronics Letters*, Vol. 33, pp. 948-949, 1997.

Papazoglou, C. A. and Karybakas, C. A., "Non-interacting electronically tunable CCII based current-mode biquadratic filters", *IEE Proc., Circuits Devices and Systems*, Vol. 144, pp. 178-184, 1997.

Piovaccari, A., “CMOS integrated third generation current conveyor”, *Electronics Letters*, Vol. 31, pp. 1228-1229, 1995.

Sagbas, M., Multifunction Filter Design Using Current Conveyors*s*, M.S. Thesis, Fatih University, 2003.

Sagbas, M. and Fidanboylu, K., "Electronically Tunable Current-Mode Second-Order Universal Filter Using Minimum Elements", *Electronics Letters*, Vol. 40, No. 1, pp. 2-4, 2004.

Sagbas, M., Fidanboylu, K. and Bayram,M.C., "Triple-input Single-output Voltage-mode Multifunction Filter Using Only Two Current Conveyors", *Electronics Letters*, Proc. of Second World Multi-Conference on Enformatika-WEC'05, pp. 105-108, 2005.

Shah N.A., Iqbal S.Z. and Rather M.F, “Versatile voltage-mode CFA-based universal filter”, Int. J. of Electron. Community, vol. 3, pp. 192-194, 2005.

Shah NA, Rather MF and Iqbal S.Z., “Three input and one output voltage-mode universal filter”, *Indian J. of Pure & Applied Physics*, Vol. 41 pp. 556-558, 2003.

Shah N.A. and Malik M.A., “High impedance voltage- and current-mode multifunction filters”, *Int. J. of Electron. Commun*, Vol. 59 pp. 262-266, 2005.

Sharma, R.K. and Senani, R, “Multifunction CM/VM biquads realized with a single CFOA and grounded capacitors”, *Int. J. Electron. Commun*, Vol. 57, pp. 301-308, 2003.

Senani, R., “New current mode biquad filter”, *International Journal of Electronics*, Vol. 73, pp. 735-742, 1992.

Senani, R., “A simple approach of deriving single-input multiple output current-mode biquad filters”, *Frequenz*, Vol. 50, pp. 124-127, 1996.

Singh, V.K. and Senani, R., “New multifunction active filter configuration employing current conveyors”, *Electronics Letters,* Vol. 26, No 21, pp. 1814-1816, 1990.

Smith, K.C. and Sedra, A., “The current conveyor: A new circuit building block”, *IEEE Proc.,* Vol. 56*,* pp. 1356-1369, 1968.

Smith, K.C. and Sedra, A., “A second generation current conveyor and its applications”, *IEEE Trans. Circuit Theory*, Vol. C.T-17, pp. 132-134, 1970.

Soliman,A. M,. “Current mode universal filter”, *Electronics letters*, Vol. 31, pp. 1420-1421, 1995.

Soliman, A. M, “New inverting non-inverting band-pass and low-pass biquad circuit using current conveyors”, *International Journal of Electronics*, Vol. 81, pp. 577-583, 1996.

Soliman,A. M,. “New filters using current conveyors”, *International Journal of Electronics and Commun. AEU*, Vol. 51, pp. 275-278, 1997.

Sun Y. and Fidler J. K., “Versatile active biquad based on second generation current conveyors”, *Int. J. Elect*., Vol. 76, No 1, pp. 91-98, 1994.

Sun, Y. and Jefferis, B. “Current-mode biquadratic filters using dual output current conveyor”, *Proc. of 5th IEEE Int. Conf. on Electron. Circuits and Syst.*, pp. 135-138, 1998.

Svoboda, J.A., McGrory, L., Webb, S., “Applications of a commercially available current conveyors”, *Int. J. Electron.,* Vol. 70, pp. 159-164, 1991.

Tangsrirat W. and Surakampontorn, W., “Realization of multiple-output biquadratic filters using current differencing buffered amplifiers”, *International Journal of Electronics,* Vol. 92, pp. 313-325, 2005.

Terzioglu, H., and Cicekoglu, O., “All-pass building blocks realized with single negative type current conveyor”, *High Voltage Techniques and Continues Time Filtering.*, pp. 325-3288, 2004.

Tiliute, E., “Second order active filter using a single current conveyor”, *International. Symp. on Signals, Circuits & Systems SCS2001,* pp. 541-542, 2001.

Toumazou, C., Lidgey, F.J. and Haigh, D.G., *Analog IC design: The Current Mode Approach,* London, Peter Pergrinus, 1990.

Weng, R.M., Lai J.R. and Lee M.H., “New universal biquad filters using only two unity-gain cells”, *Int. J. of Electronics*, Vol. 87, pp. 57-61, 2000.

Wandsworth, D.C., “Accurate current conveyor topology and monolithic implementation”, *IEE Proc. G*, Vol. 2, pp. 88-94, 1990.

Wilson, B., “Recent developments in current mode circuits”, *Proc. IEE Proc. G*, Vol. 137, pp. 63-67, 1990.